

52

~~CONFIDENTIAL~~
~~RESTRICTED DATA~~
~~Atomic Energy Act of 1954~~



WANL-TME-744

APRIL, 1964

WESTINGHOUSE ELECTRIC CORPORATION
ASTRONUCLEAR LABORATORY
PITTSBURGH 36, PENNSYLVANIA

MASTER

By:

R. B. Phillips
R. B. Phillips

G. E. Cort
G. E. Cort

Approved:

A. Bournia
A. Bournia - Supervisor

Approved:

J. G. Gallagher
J. G. Gallagher
Acting Manager
Reactor Analysis

~~INFORMATION CATEGORY
Confidential RD
A. Bournia 13-64
Authorized Classifier Date~~

Classification cancelled (or changed to _____)
by authority of _____
by K. J. C. TIC, date **SEP 11 1973**

**SPECIAL REREVIEW
FINAL
DETERMINATION**
Class: U
Reviewer: KAW Class: U Date: 5-11-82

THERMAL ANALYSIS OF HIGH TEMPERATURE
FUEL ELEMENT CORROSION TESTS
(Title Unclassified)

DISTRIBUTION OF THIS DOCUMENT IS UNLIMITED

NOTICE
This report was prepared as an account of work sponsored by the United States Government. Neither the United States nor the United States Energy Research and Development Administration, nor any of their employees, nor any of their contractors, subcontractors, or their employees, makes any warranty, express or implied, or assumes any legal liability or responsibility for the accuracy, completeness or usefulness of any information, apparatus, product or process disclosed, or represents that its use would not infringe privately owned rights.

Excluded From Automatic Downgrading
and Declassification

DISCLAIMER

This report was prepared as an account of work sponsored by an agency of the United States Government. Neither the United States Government nor any agency Thereof, nor any of their employees, makes any warranty, express or implied, or assumes any legal liability or responsibility for the accuracy, completeness, or usefulness of any information, apparatus, product, or process disclosed, or represents that its use would not infringe privately owned rights. Reference herein to any specific commercial product, process, or service by trade name, trademark, manufacturer, or otherwise does not necessarily constitute or imply its endorsement, recommendation, or favoring by the United States Government or any agency thereof. The views and opinions of authors expressed herein do not necessarily state or reflect those of the United States Government or any agency thereof.

DISCLAIMER

Portions of this document may be illegible in electronic image products. Images are produced from the best available original document.

~~CONFIDENTIAL~~
~~RESTRICTED DATA~~
~~Atomic Energy Commission~~



WANL-TM.E-744

ABSTRACT

An analysis of the fuel element corrosion test (test A-2) of the NRX-A component test program has been made. Calculated results are presented which show the temperature distribution in the fuel elements and the flow rate, temperature, and pressure distribution of the hydrogen in the coolant channels, for standard test conditions. A comparison is made between calculated and measured results to partially verify the analytical approach used in the thermal design of the NRX-A reactors. A comparison of the fuel element thermal and flow characteristics in the corrosion test and the NRX-A2 is presented. Modifications to the test hardware, instrumentation, and operating conditions are recommended to better verify the heat transfer analysis of the fuel element corrosion test.

~~CONFIDENTIAL~~
~~RESTRICTED DATA~~
~~Atomic Energy Commission 1954~~

~~CONFIDENTIAL~~
~~RESTRICTED DATA~~



WANL-TME-744

SUMMARY

The detailed temperature distributions which have been calculated for the standard corrosion test conditions are presented. If the proper heat loss from the element is assumed, good agreement between calculated and measured values are obtained. Within the limitations imposed by assuming a heat loss, the corrosion test data confirm the analytical methods within the test range investigated.

The major difference between the conditions of the corrosion test and of the nominal NRX-A conditions is the axial shape of the heat generation curve. The corrosion test has its peak generation at the hot end while the NRX-A will have peak generation at mid span. The total generation in the two systems are similar, as are the flow conditions of the hydrogen coolant. The shape of the heat generation in the corrosion test causes the maximum material temperature to be higher than nominal NRX-A material temperature.

~~CONFIDENTIAL~~
~~RESTRICTED DATA~~

CONFIDENTIAL

RESTRICTED DATA



TABLE OF CONTENTS

	<u>Page No.</u>
Abstract	i
Summary	ii
Table of Contents	iii
List of Tables	iv
List of Figures	v-vi
Nomenclature	vii
1.0 Introduction	1
2.0 Apparatus and Instrumentation	2
3.0 Analytical Procedure	4
4.0 Discussion	6
4.1 Test Description	6
4.2 Test Analysis	7
5.0 Results	9
5.1 Calculated Results	9
5.2 Comparison to Measured Results	9
5.3 Comparison to NRX-A Conditions	12
6.0 Recommendations	13
7.0 References	14

CONFIDENTIAL

RESTRICTED DATA

LIST OF TABLES

<u>Table No.</u>		<u>Page No.</u>
I	Hydrogen Temperature and Flow Distribution for 4460 °R Set Temperature (Test 1B)	15
II	Measured Heat Transfer Coefficients	16
III	Comparison of Several Heat Transfer Correlations Evaluated at the Conditions of the Component Test	17
IV	Measured Pressure Drop	18

LIST OF FIGURES

<u>Figure No.</u>		<u>Page No.</u>
1	Single Element Hydrogen Corrosion Furnace	19
2	High Temperature Test Cell	20
3	Schematic Drawing of the Test Rig and Instrumentation	21
4	TOSS Nodal Model Used for Analysis of the Fuel Element Between Chucks	22
5	Three Dimensional TOSS Model for End Temperature Calculation	23
6	Electrical Resistivity of Graphite G vs. Temperature	24
7	Normalized Axial Heat Generation for Electric Heating	25
8	Effect of Assumed Heat Loss on Calculated Surface Temperature	26
9	Distribution of Heat Loss for 4460° Set Temperature (Test 1B)	27
10	Temperature Distribution at Axial Locations for 4320 °R Set Point (Test 1C)	28
11	Temperature Distribution at Axial Locations for 4460 °R Set Point (Test 1B)	29
12	Temperature Distribution at Axial Locations for 4600 °R Set Point (Test 1A)	30
13	Maximum Calculated Temperature Difference Along the Element	31
14	Calculated Axial Temperature Distribution for 4320 °R Set Point (Test 1C)	32
15	Calculated Axial Temperature Distribution for 4460 °R Set Point (Test 1B)	33
16	Calculated Axial Temperature Distribution for 4600 °R Set Point (Test 1A)	34
17	Comparison of Measured to Calculated Surface Temperature	35
18	Calibration of Optical Pyrometers	36
19	Temperature Gradient on an Axial Cross Section of a Fuel Element	37
20	Comparison of Calculated Temperature Variance to Variance Measured by Material Analysis	38

LIST OF FIGURES
(continued)

<u>Figure No.</u>		<u>Page No.</u>
21	Comparison of Measured and Calculated Pressure Drop	39
22	NRX-A Heating Rates Compared to Electrical Heating at 4600 °R Set Point	40
23	NRX-A Design Axial Temperature Distribution, F.Q. = 1.0	41
24	Component Test Axial Temperature Distribution for 4320 °R Set Temperature (Test 1C)	42
25	Velocity and Pressure Distribution for Component Test and For Nominal NRX-A	43

NOMENCLATURE

- h = heat transfer coefficient, BTU/hr ft °F
- D = diameter of flow channel, in.
- k = thermal conductivity, BTU/hr ft °F
- (N_{Re}) = Reynolds' Number
- (N_{Pr}) = Prandlt Number
- T = Temperature, °R
- X = length from inlet, in.
- γ = kinetic viscosity

Subscripts

- b = bulk
- f = film (avg. of wall and bulk properties)
- w, s = wall
- x = local

1.0 INTRODUCTION

The component test program for NRX-A reactors is described in Reference (1). This program includes a fuel element component flow test (test A-2), in which fuel elements are heated to a high temperature. The test is conducted to simulate core conditions expected in the NRX-A core. In this test, a voltage is applied across the length of the element and electrical power appears as heat in the element. Hydrogen flows through the coolant channels of the element and is heated to a high temperature.

The major objective of the test is to measure the quality of fuel elements by investigating the resistance to hydrogen corrosion offered by fuel element coatings and the overall ability of elements to withstand high temperature. A secondary objective of the test is to confirm the analytical methods used in the thermal design of NRX-A reactors.

The tests performed to date have been confined largely to test rig debugging and quality control testing. The test operating conditions and test instrumentation have been aimed at fulfilling this function rather than providing a wide range of test variables with complete instrumentation as required for confirmation of analytical methods.

A thermal and fluid flow analysis of the fuel element quality control tests has been performed to define temperature distribution throughout the element and the hydrogen temperature, pressure, and mass flow distribution within the element. A comparison of this analysis to values measured in the quality control tests gives a preliminary check on the method of analysis. This report presents the results of the fuel element component test analysis.

2.0 APPARATUS AND INSTRUMENTATION

The test apparatus consists of a water cooled furnace in which the fuel element is held between graphite chucks. A helium atmosphere is provided in the furnace at a pressure higher than the hydrogen inlet pressure. The graphite chucks provide electrical contact to the fuel element and are a seal to prevent mixing of the hydrogen coolant and the helium atmosphere.

A complete and detailed description of the apparatus and its operation has been reported in Reference (2). Figures 1 and 2 are reproduced from Reference (2) and show a photograph of the installed apparatus and a cross section of the water cooled furnace.

The instruments which measure the parameters used in the heat transfer analysis are the optical pyrometers, gas flow rate measuring devices, the pressure gauges, and the volt and ampere meters from which the test power is determined. Figure 3 is a schematic diagram of the apparatus and the installed instrumentation.

The micro-optical pyrometers are used to measure the external surface temperature of the fuel element at the 3.5 in., 15.5 in., 38 in., and 48.5 in. stations, measuring from the inlet of the element. These pyrometers have been calibrated in place so that the reported temperatures include a correction for absorptivity of the view path. The instruments are reportedly capable of sensing $\pm 10^{\circ}$ temperature variation in the range of 3500°R to 5000°R and $\pm 30^{\circ}\text{R}$ at 2500°R . The pyrometers are not capable of sensing temperatures below 1660°R .

~~CONFIDENTIAL~~
~~RESTRICTED DATA~~



The hydrogen flow rate is measured upstream of the element with a calibrated Daniels' orifice. The pressure drop across the orifice is measured with a pressure transducer which has sensitivity to detect a 1% change in flow. The hydrogen temperature at the orifice is also measured.

Hydrogen pressure at the furnace discharge is measured with a bourdon tube pressure gauge of 5 psi sensitivity. Pressure drop is measured with a ΔP transducer.

The test power is measured across the power supply and across the furnace with an ampere meter and voltage meters. The sensitivity of these are sufficient to detect $\pm 3\%$ change in power.

A great many additional measurements (Reference (2)) are made in order to control the test, protect equipment, and assure safe operation.

~~CONFIDENTIAL~~
~~RESTRICTED DATA~~

3.0 ANALYTICAL PROCEDURE

The analysis of the test cases was done in two parts. The first part included the section of the element between the chucks but not within the chucks. The second part was an analysis of the element within the hot end chuck.

The solution for the temperature distribution between the chucks was obtained using the TOSS⁽³⁾-MCAP⁽⁴⁾ digital computer codes. As stated in Reference (5), TOSS is a program for finding the transient or steady state temperature distribution of a one, two, or three dimensional irregular body. It considers the heat transfer mechanisms of conduction between internal nodes, conduction between internal and surface nodes, radiation between surface points, and radiation, free convection and forced convection between surface and boundary points. MCAP is a steady state, hydraulic and convective heat transfer program which is used in determining the flow distribution through a multi-channeled flow system with heat addition. It is used to determine the fluid pressure and temperature distribution and coolant channel wall temperature in a heat generating solid which is cooled by a gas flowing in parallel channels.

The codes were set up to describe the geometry and physical properties of the fuel element and the hydrogen. The heat transfer correlation recommended in Reference (6) was used in MCAP. The input to the codes included the hydrogen flow rate (0.0443 lb/sec), inlet temperature (530 °R), exit pressure (560 psig), power generation shape (discussed later), and a power generation level which was adjusted to give the desired surface temperature at the 48.5 in. length. The heat flux from the external surface of the element was adjusted to simulate heat loss by radiation to the shields and convection to the helium atmosphere.

The fluid conditions and wall temperature of each coolant channel was calculated at 2 in. intervals along the element in the MCAP program. The channel wall temperatures and the heat fluxes were calculated in the TOSS program at 5 axial stations along the element. A convergence between TOSS and MCAP was obtained when the heat fluxes and wall temperatures from both programs was the same at the five stations.

The program output gave the temperature at the nodal points of the TOSS model, Figure 4, at each of the 5 axial positions, thus defining the temperature distribution throughout the element. Other output included the overall coolant pressure drop and the distribution of pressure and temperature in the coolant channels.

The analysis of the part of the fuel element contained in the hot end chuck was done in the TOSS program only. An estimate of the fluid conditions were obtained from the analysis of the rest of the fuel element. Changes in temperature of the coolant due to inter-change of heat among channels was neglected. An analysis of the calculated results indicated that the effects of the inter-change of heat among channels was small. The TOSS model used for this analysis is given in Figure 5.

4.0 DISCUSSION

4.1 Test Description

The quality control tests of fuel elements is carried out by the Fluid Flow Laboratory at WANL. The tests have consisted of setting a hydrogen flow rate through the element of 500 SCFM with a controlled back pressure of 560 psig. The test power is increased in steps until the predetermined fuel element surface temperature is obtained at the pyrometer sight port located 48.5 in. from the cold end. This temperature is maintained, by adjusting power, for the duration of the test, usually 5 minutes. The power is then reduced to zero in steps and the test terminated.

Standard tests have been defined which consist of setting given temperatures at the 48.5 in. sight port with the 500 SCFM hydrogen flow rate and 560 psig back pressure. The standard test temperatures have been 4600 °R (test 1A), 4460 °R (test 1B) and 4320 °R (test 1C). Analyses have been conducted for each of these set temperatures.

During each test, the following measurements are recorded. Typical data for test runs is indicated:

- | | |
|---|----------|
| (1) Element surface temperature at 48.5 in. from cold end | 4460 °R |
| Element surface temperature at 38 in. from cold end | 3800 °R |
| Element surface temperature at 15.5 in. from cold end | 2850 °R |
| Element surface temperature at 3.5 in. from cold end | >1600 °R |
| (2) Inlet hydrogen pressure | 660 psig |
| (3) Exit hydrogen pressure | 560 psig |
| (4) Voltage | 200 |

(5) Current	400 amps.
(6) Helium flow rate	35 SCFM
(7) Hydrogen flow rate	500 SCFM
(8) Hydrogen inlet temperature	Ambient
(9) Start up time	45 secs.
(10) Time at steady state	5 min.
(11) Cool down time	45 sec.

The test procedure is described in greater detail in Reference (2).

4.2 Test Analysis

The solution for the temperature distribution of the test cases was obtained using the TOSS-MCAP digital computer codes described in Section 3.0. An important input to the programs to be determined is the shape of the heat generation curve.

With electrical heat generation, the shape of the power generation curve is a function of the variation in electrical resistance along the fuel element. The shape of the power generation curve is not a controllable part of the test and in this respect the test does not simulate reactor power. The local electrical resistance is a strong function of temperature, as shown in Figure 6 from Reference (7). The calculation for material temperature is a trial and error solution in which the material temperature and the heat generation shape are mutually dependent. Figure 7 shows a normalized power generation curve that has been obtained in the solution of one of the test cases.

An unknown factor in the analysis is the heat loss from the element surface by radiation and by convection to the helium atmosphere. At the test conditions, part of

the total heat generated is lost to the surroundings and the calculated values depend on what heat loss is used, Figure 8. Four different heat losses were considered during the analysis - zero heat loss, radiation with a 0.7 form factor, radiation with a 1.0 form factor, and radiation plus a convective heat loss. In the last case the radiation was for a black body (the fuel element) radiating to a perfect sink at the radiation shield temperature and the convection was equivalent to the measured helium flow being in thermal equilibrium with the fuel element surface at every axial position. The heat loss and the distribution of the heat loss along the element were thus specified. Calculated values depend on both the total heat loss and on the distribution of the loss along the element. The heat loss obtained by this assumption is shown in Figure 9 as a function of length, along with the integrated value. It has been found that the surface temperatures calculated using this latter assumption for heat loss gave the best possible fit of the measured data for every power input and at both lengths where good measured temperatures are available. The present calculations are, however, limited by this assumption. Experimental data is needed to confirm the heat loss calculations.

5.0 RESULTS

5.1 Calculated Results

Using the calculated heat generation shape and the heat loss as discussed, the temperature distribution within the element upstream of the chuck was calculated for the standard test conditions. These results are shown in Figures 10, 11 and 12. Also shown are the calculated temperatures for the end face of the element. The maximum variation in temperature at all points along the element is given in Figure 13 for the three test conditions.

Figures 14, 15 and 16 show the calculated surface temperature, maximum material temperature, and average hydrogen temperature along the element. Table I shows the hydrogen exit temperature distribution and the flow distribution among the coolant channels for a standard test condition, test 1B.

5.2 Comparison to Measured Results

A comparison is made in Figure 17 of the calculated electrical power and the measured power at points along the element. Note that the analysis at 15.5 in. length does not fit the data. One explanation for the poor fit becomes apparent from the pyrometer calibration curve in Figure 13. Data in the range measured at the 15.5 in. length depends on extrapolating two curves whose slopes are changing rapidly. A new calibration in this temperature range is planned.

The data-fit at the two other test lengths, 38 and 48.5 inches, is excellent and seems to confirm the present assumptions for heat loss. (The data at 15.5 in. cannot be made to fit with any heat loss greater than zero).

The calculated surface temperature for a given power input depends on the value used for the heat transfer coefficient of the coolant in the channels and on the heat lost from the surface. Since the calculated surface temperature fits the measured data it is implied that the hydrogen heat transfer coefficients achieved in the test are the same as those used in the analysis if the assumed heat loss is correct. It is of interest, nevertheless, to show the heat transfer coefficient which is necessary to cause the calculated surface temperature to match the measured power for each individual test run, with the heat loss specified as discussed. Table II gives this comparison at the 38 in. and 48.5 in. stations for the test data. As indicated, the comparison to the analysis is quite good.

Table III gives the heat transfer coefficients calculated by the empirical heat transfer correlation used in this analysis along with the average of those used to fit the measured data. Several other correlations are also shown. It is noted that there is not a significant variation among the various correlations (neglecting one) when evaluated at the test conditions.

Estimates of the temperature distribution obtained in fuel elements during corrosion tests have been made by post-mortem material analysis as reported in Reference (8). This method consists of comparing (at high magnification) the interaction of the fuel beads with the NbC liner in corrosion tests to the interaction obtained in control specimens for which the operating temperature was known. The accuracy of the measurement was thought to be not better than $\pm 90^\circ \text{R}$. Figure 19 shows a comparison of the temperature distribution measured by material analysis to the calculated distribution at points

along the element. In this figure, only the shapes of the gradients should be compared since the temperature levels are not the same for the two methods. Fair agreement is obtained

Figure 20 shows a comparison, for various operating conditions, of the two methods of obtaining the temperature variation. In this curve, the comparison is made at the hot end. For the material analysis, the uncertainty of the data is indicated. Since this method depends upon the interaction of the NbC with the uranium fuel, the temperature measured applies to the interface of the NbC with the fuel. The comparable calculated temperature is the wall temperature of the coolant channel. The calculated variation is shown for both the maximum web temperature and the wall temperature of the center coolant channel. In addition, the internal web temperature was measured for one operating condition by sighting an optical pyrometer to the bottom of a hole drilled into the center of the fuel element. This data point is also shown on the curve. Note that the measured internal temperature causes the point to fall close to the calculated curve.

Another result of the analysis is a comparison of the measured to calculated pressure drop. Table IV is a tabulation of the measured pressure drop for a group of test runs. Unfortunately, the channel diameters were not known for the fuel elements in this test. However, a group of fuel elements manufactured by the identical process and at about the same time were found to have equivalent channel diameters varying from 0.093 in. to 0.098 in. and averaging approximately 0.0955 in. Figure 21 shows the calculated pressure drop for elements with .095 in and .0965 in. equivalent diameter for the

test runs at various test surface temperatures. The effect of surface roughness has been factored into the calculation. The average of the measured values is shown and the scale of the data scatter is indicated. If the actual diameters of the test elements were near .0955 in., then the comparison is quite good.

5.3 Comparison to NRX-A Conditions

The major difference between the electrical tests and the NRX-A hot conditions is the shape of the heat generation curve. Figure 22 gives a comparison of the NRX-A heat generation rates to those obtained in the electrical test. It is noted that for the same total power the peak heat generation is higher in the electrical test than in the NRX-A, though the peak is displaced. Figure 22 also shows the peak heat generation of the quality control test at 4600 °R surface temperature exceeds the peak generation anticipated in the NRX-A reactor.

Figures 23 and 24 show material and fluid temperatures along the element for the NRX-A at nominal conditions and for the quality control test at the same outlet temperature. Note that the maximum material temperature in this test is 620 °R higher than the nominal material temperature in the NRX-A. This difference is due in part to the shape of the heat generation curve and also to the heat loss from the element surface.

The velocity and pressure distributions achieved in the quality control test are quite similar to those of the NRX-A reactor as shown in Figure 25. It is noted that the 500 SCFM flow rate of the quality control tests is .0443 lb/sec per element compared to the nominal NRX-A flows of 0.0413 lb/sec per element.

6.0 RECOMMENDATIONS

1. A wider range of test parameters is required to confirm the heat transfer coefficient. Specifically the following test conditions are recommended:

- | | |
|-----------------------------------|-------------------------|
| (a) Coolant Flow Rate | 100 to 800 SCFM |
| (b) Coolant exit temperature | 1000 °R to 4700 °R |
| (c) Discharge Pressure | 2 ATM to facility limit |
| (d) Surface temperature (hot end) | 1000 °R to 5000 °R |

2. More complete instrumentation is required to better understand the test and to improve heat transfer verifications. Specifically the following additional measurements are recommended.

- (a) Material temperatures at selected points in the element.
- (b) Coolant temperature-inlet and exhaust of the element.
- (c) Environmental temperatures-shield, helium atmosphere, and chuck.

3. A heat balance for the entire system.

4. Modify the test equipment in order to give end conditions comparable to the reactor condition.

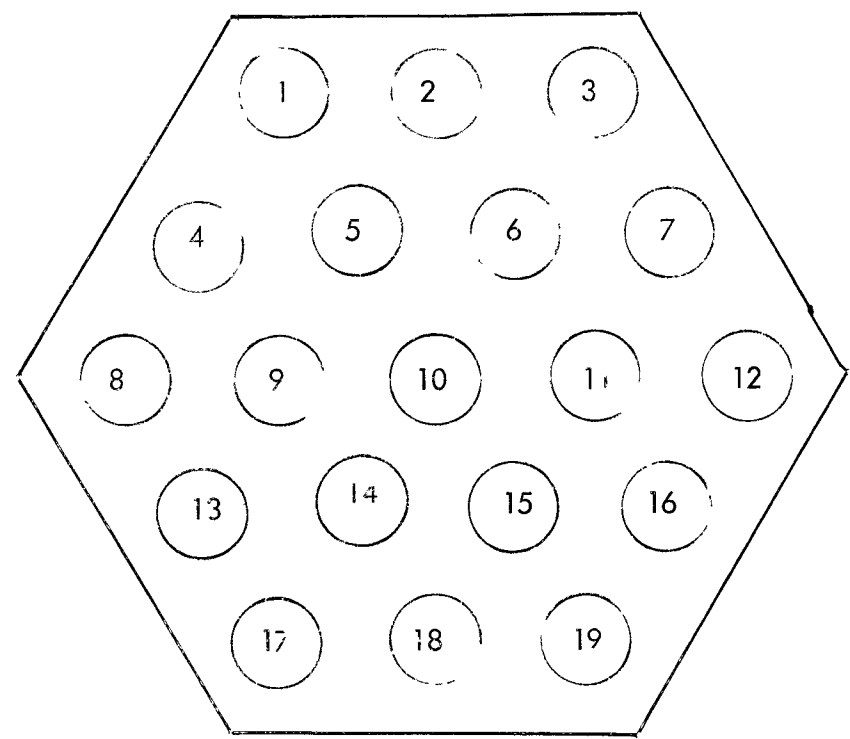
jcb

7.0 REFERENCES

1. "NRX-A Component Test Program, Block I," WANL-TNR-095 (Revised) (July, 1963).
2. R. D. Foster and R. R. Burghardt, "High Temperature Testing of Pre-Production Fuel Elements," WANL-TME-502 (September, 1963).
3. David Bagwell, "TOSS An IBM - 7090 Code for Computing Transient or Steady State Temperature Distributions," K-1494, Union Carbide Nuclear Company (December, 1961).
4. B. L. Pierce, "A Multiple Channel Analysis Program (MCAP) for the Temperature Distribution in an Internally-Cooled Heat Generating Solid Cooled by a Compressible Gas," WANL-TMI-117 (March, 1962).
5. "Reactor Analysis of NRX-A Thermal and Fluid Flow Analysis," WANL-TNR-128, Vol. III (September, 1963).
6. G. R. Thomas, "An Interim Study of Single Phase Heat Transfer Correlations Using Hydrogen," WANL-TNR-056 (April, 1962).
7. "Materials for Design," WANL-TNR-022 (March, 1962).
8. M. B. Blinn, "Hydrogen Corrosion Testing of NERVA Reference Fuel," WANL-TNR-129 (September, 1963).
9. W. R. Thompson and E. L. Geery, "Heat Transfer to Cryogenic Hydrogen at Supercritical Pressures," Aerojet Rept. 1842 (July, 1960).
10. M. F. Taylor, "Local Heat Transfer Measurements for Forced Convection of Hydrogen and Helium at Surface Temperatures up to 5600 °R," Lewis Research Center, National Aeronautics and Space Administration.
11. K. Williamson, during SNPO Meeting on Hydrogen Heat Transfer Coefficients at Los Alamos Scientific Laboratory, Los Alamos, New Mexico, January 29, 30, 1964.

TABLE I

HYDROGEN TEMPERATURE AND FLOW DISTRIBUTION FOR
 4460 °R SET TEMPERATURE (TEST 1B)



	Channel No. 10	Channel No. 1, 3, 8, 12, 17, 19	Channel No. 2, 4, 7, 13, 16, 18	Channel No. 5, 6, 9, 11, 14, 15
H ₂ Flow Rate/Channel, lb/sec	.00229	.00235	.00234	.0023
H ₂ Discharge Temp. °R	4487	4214	4258	4407

CONFIDENTIAL
RESTRICTED DATA



TABLE II
 MEASURED HEAT TRANSFER

Set Temperature - 4460 °R			Set Temperature - 4600 °R		
Run No.	Heat Transfer Coefficient		Run No.	Heat Transfer Coefficient	
	Btu/hr ft ² °R			Btu/hr ft ² °R	
	48.5 in.	38 in.		48.5 in.	38 in.
207	2348	2679	212	4281	3260
208	3599	2722	215	3158	
209	6078	3593	217		4069
210	3257	2824	218	4728	3484
213	2771	2696	219	3344	2622
214	2530	2428	220	4641	3323
216	4806		221	3071	2826
226	2406	2539	222	3578	2993
229	3746	3253	223		3245
230	3515	2508	224	2526	2315
231	2716	2492	225		3903
232	3627	2687	227	3871	2638
233	3408	3063	228	3749	2577
234	2482	2844	238	3158	2501
235	3686	2885	241	4136	3910
236	5433	3140	242	2724	2670
237	3808	3458			
240	3257	2663			
243	2498	2200			
244	3570	2655			
245	2452	2995			
Average	3183	2816	Average	3613	3089
Calculated*	3171	2814	Calculated*	3493	2869

* Recommended heat transfer correlation, WANL-TNR-056

CONFIDENTIAL
RESTRICTED DATA
 Atomic Energy Act - 1954

TABLE III

COMPARISON OF SEVERAL HEAT TRANSFER CORRELATIONS EVALUATED AT THE CONDITIONS OF THE COMPONENT TEST

Distance From Inlet in.	Avg. of Component Test 1B	Recommended Ref (6) (1)	Ref (9) (2)	Ref (9) (3)	Ref (9) (4)	Ref (10) (5)	Ref (10) (6)	Ref (11) (7)
2		1539	1580	1460	731	1383	1543	1822
10		2052	2197	1916	922			
30		2598	2862	2346	1092			
38	2816	2816	3111	2524	1092			
48	3183	3171	3515	2818	1180	2843	3942	3072

$$(1) \quad (hD/k)_b = .025 (N_{Reb})^{.8} (N_{Prb})^{.4} (T_w/T_b)^{-.55} \left[1 + .3(x/d)^{-.7} \right]$$

$$(2) \quad (hD/k)_b = .028 (N_{Reb})^{.8} (N_{Prb})^{.4} (T_w/T_b)^{-.64}$$

$$(3) \quad (hD/k)_b = .0217 (N_{Reb})^{.8} (N_{Prb})^{.4} (T_w/T_b)^{-.34}$$

$$(4) \quad (hD/k)_b = .000534 (N_{Reb})^{1.1} (N_{Prb})^{.4} (T_w/T_b)^{-.64}$$

$$(5) \quad (hD/k)_f = .021 (N_{Ref})^{.8} (N_{Prf})^{.4} (T_f/T_b)^{-.8}$$

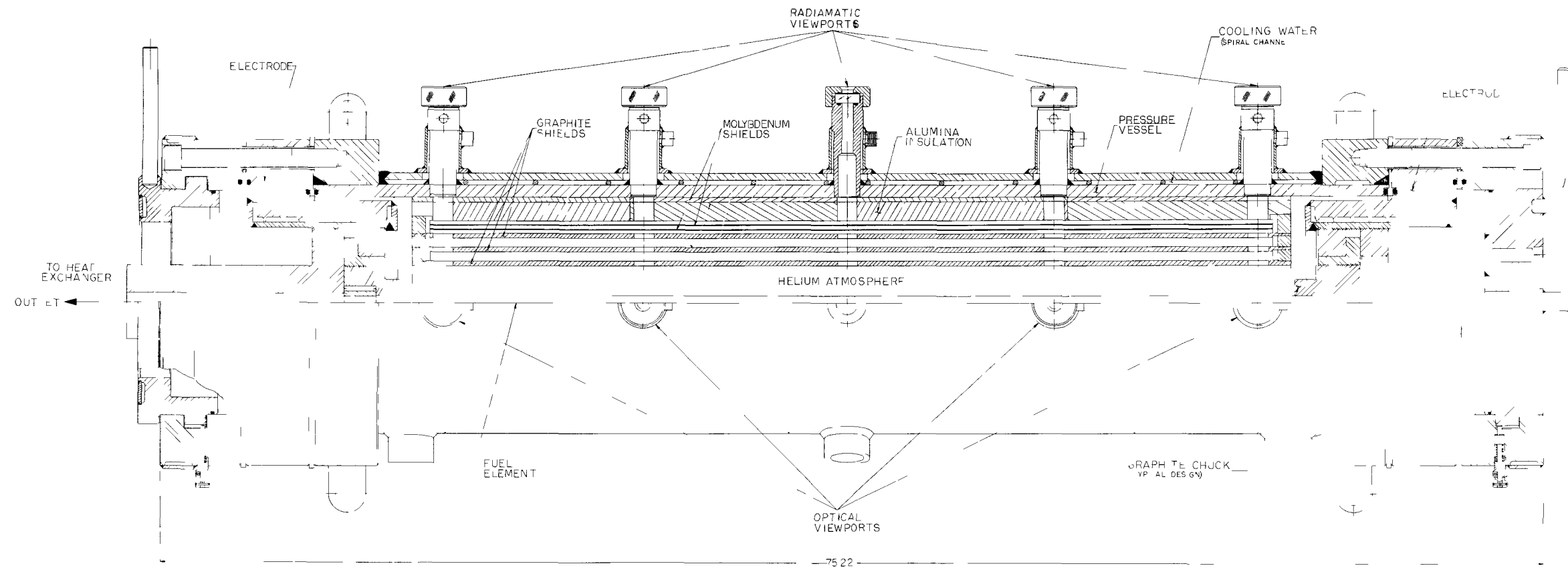
$$(6) \quad (hD/k)_s = .0265 (N_{Res})^{.8} (N_{Prs})^{.4} (T_s/T_b)^{-.8}$$

$$(7) \quad (hD/k)_f = .0208 (N_{Ref})^{.8} (N_{Prf})^{.4} (1 + 0.01457 \gamma_s / \gamma_b)$$

TABLE IV

MEASURED PRESSURE DROP

Set Temperature - 4460 °R		Set Temperature - 4600 °R	
Run No.	$\Delta P_{\text{Measured}}$ lb/in ²	Run No.	$\Delta P_{\text{Measured}}$ lb/in ²
207	84	211	82
208	90	212	97
209	103	215	61
210	87	217	102
213	94	218	105
214	92	219	104
216	120	220	108
226	93	221	98
229	97	222	105
230	91	223	106
231	91	224	92
232	86	225	114
233	100	227	106
234	85	228	104
235	98	238	98
236	96	241	103
237	103	242	100
240	96		
243	84		
244	90		
245	86		
Average	93.6	Average	102.8
Calculated	97	Calculated	102



SINGLE ELEMENT HYDROGEN CORROSION FURNACE

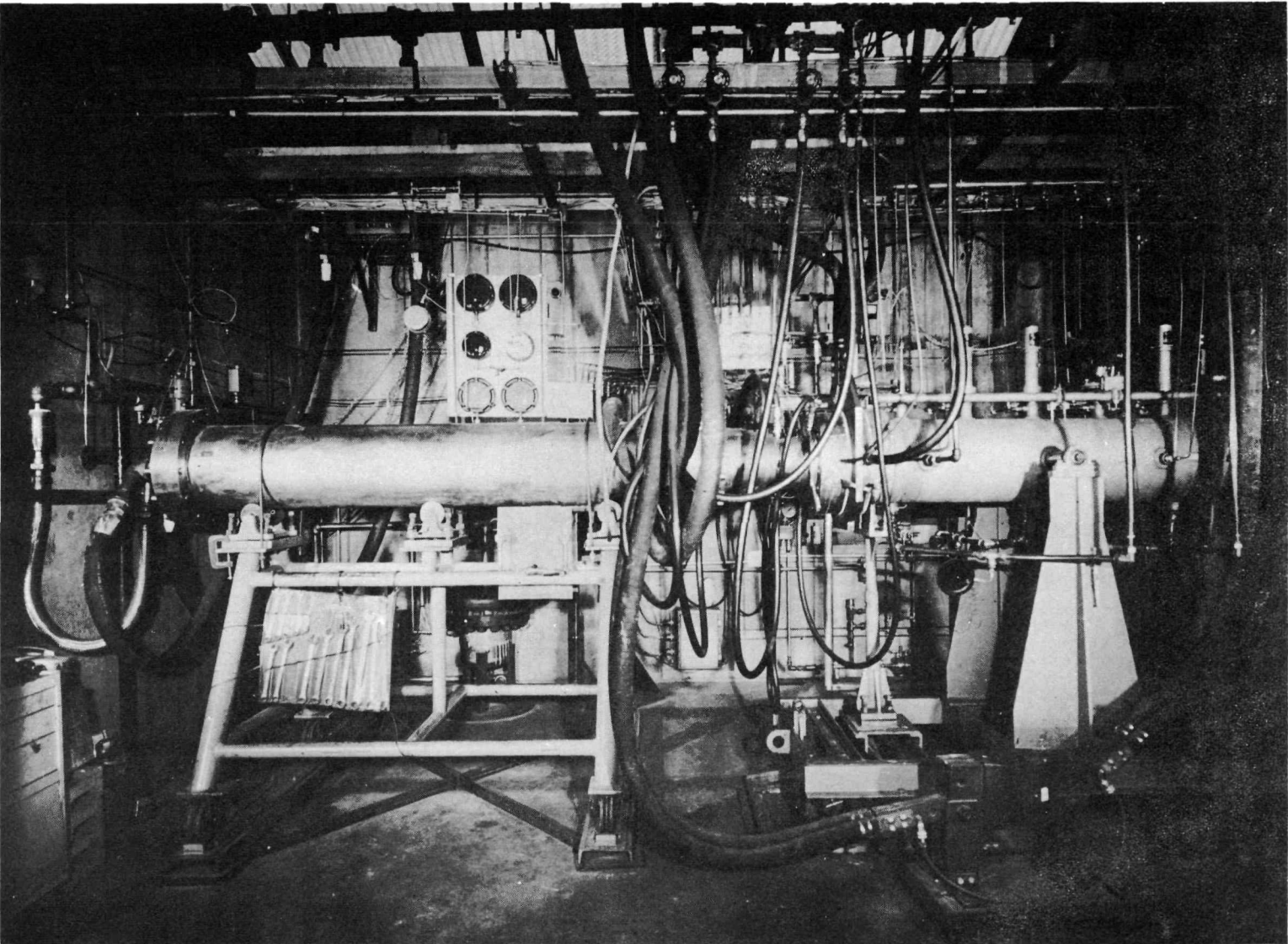
FIGURE 1



CONFIDENTIAL
RESTRICTED DATA
Atomic Energy Act - 1954



FIGURE 2
HIGH TEMPERATURE TEST CELL



CONFIDENTIAL
RESTRICTED DATA
Atomic Energy Act - 1954

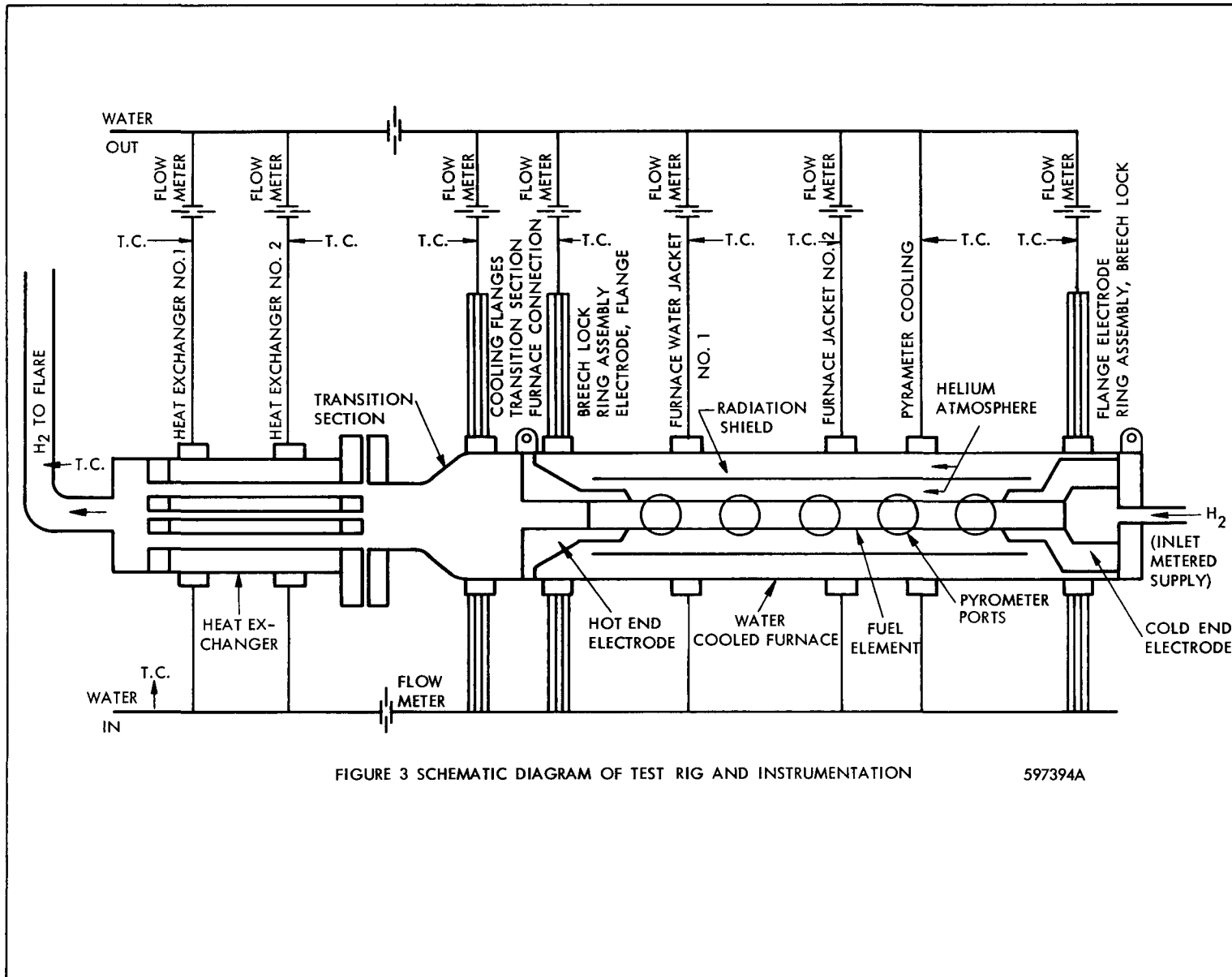



FIGURE 3 SCHEMATIC DIAGRAM OF TEST RIG AND INSTRUMENTATION

597394A

REFERENCE		PREPARED BY <i>WCP</i>	APPROVED BY <i>AB</i>	 Astronuclear
-----------	--	---------------------------	--------------------------	--

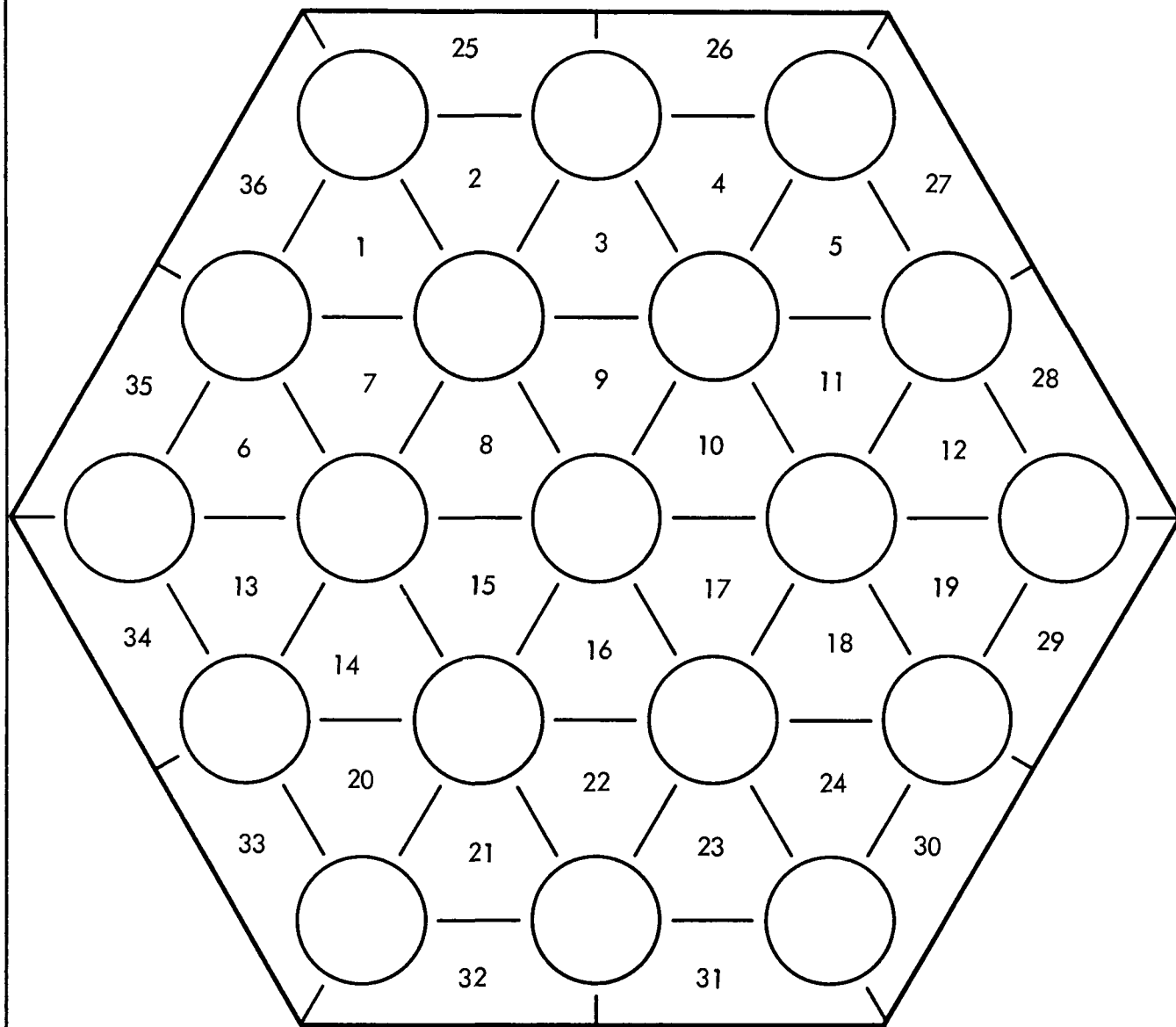


FIGURE 4 TOSS NODAL MODEL USED FOR ANALYSIS OF THE FUEL ELEMENT BETWEEN CHUCKS

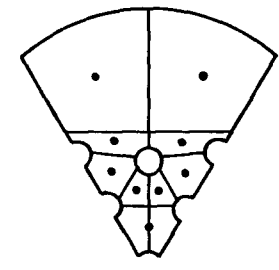
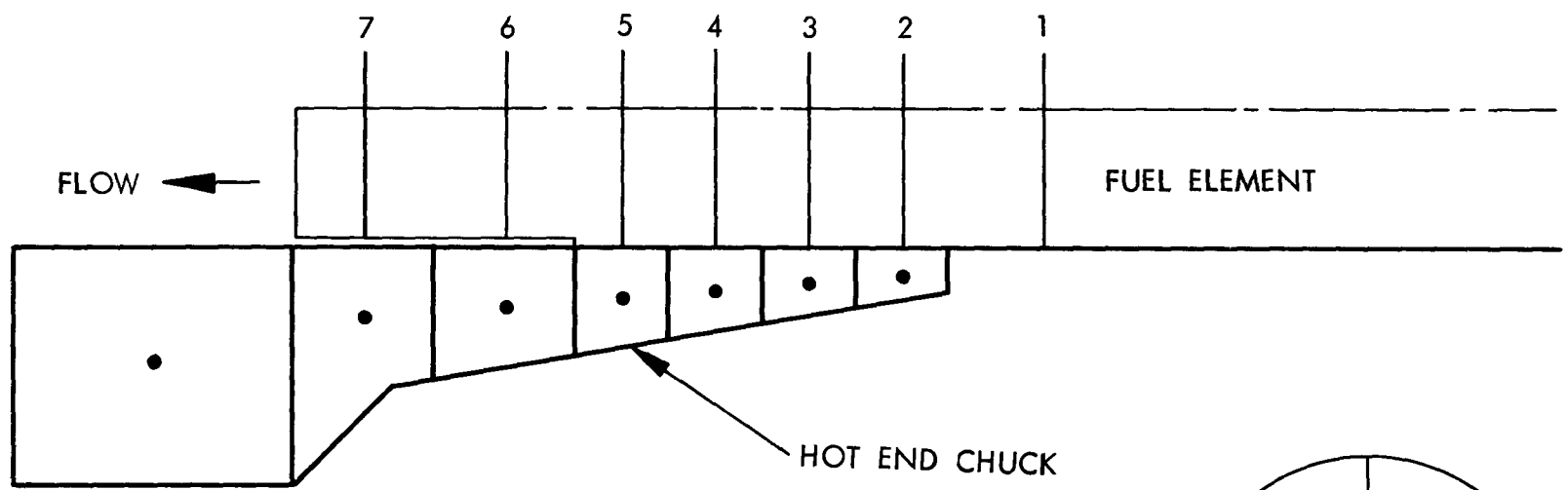
INDEX NO.

597400 A

REFERENCE

 Astronuclear

1954



SECTION 5

INDEX NO.

FIGURE 5 THREE-DIMENSIONAL TOSS MODEL FOR END TEMPERATURE CALCULATION

PREPARED BY

GP

APPROVED BY

GP

CURVE NO.

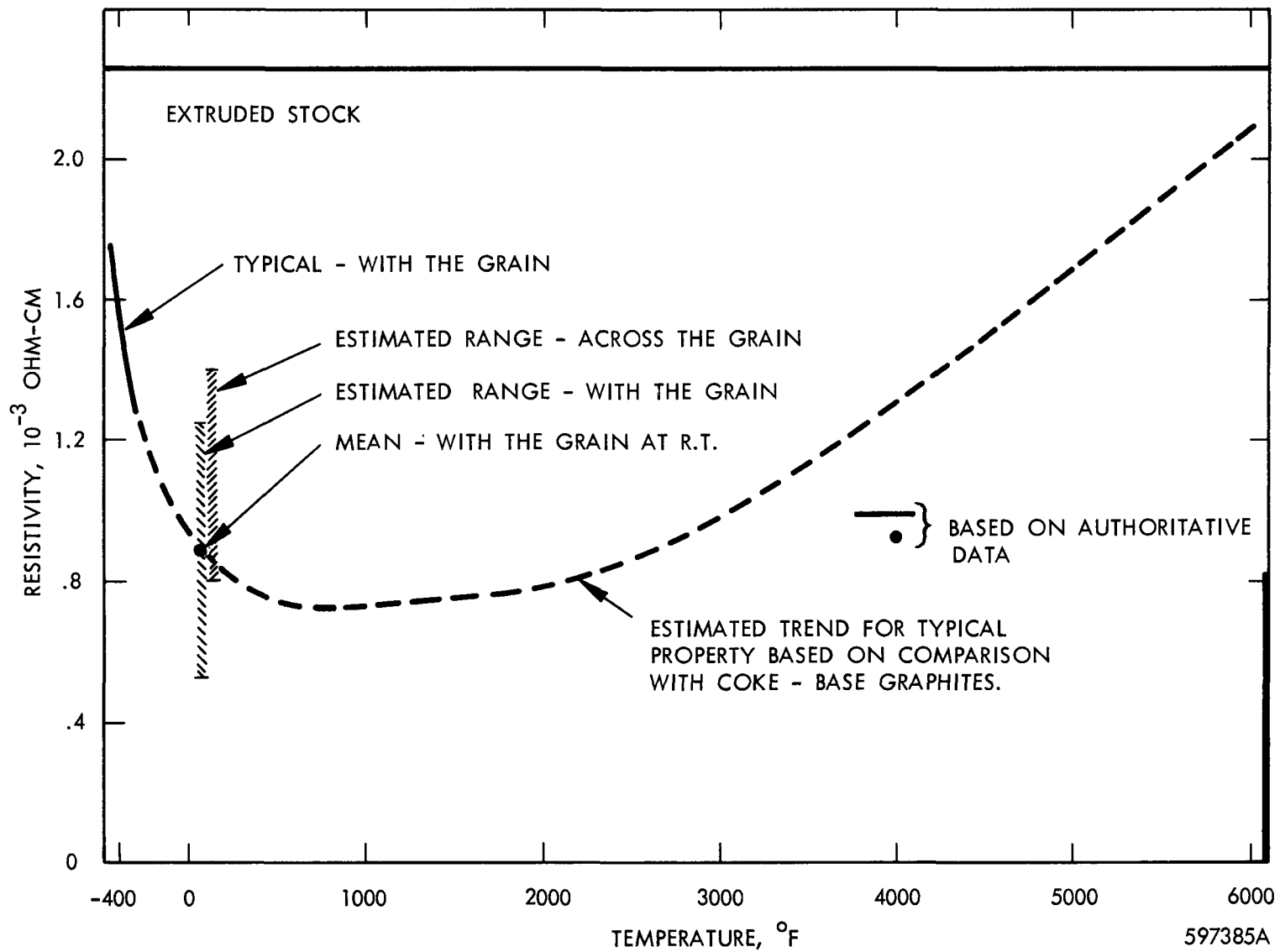
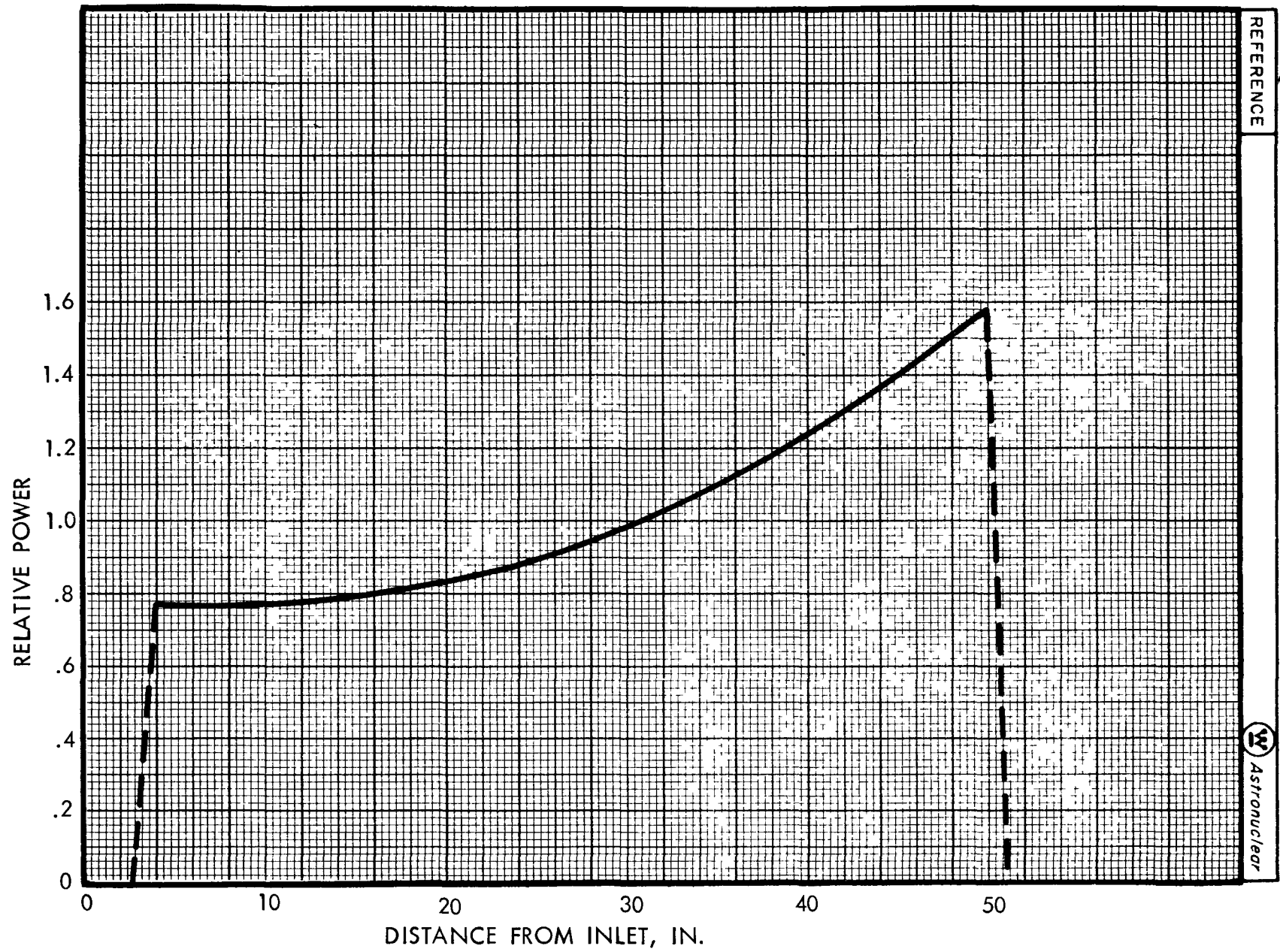


FIGURE 6 ELECTRICAL RESISTIVITY OF GRAPHITE G VS TEMPERATURE

597385A

CONFIDENTIAL UNCLASSIFIED DATA Atomic Energy Act of 1954

CONFIDENTIAL UNCLASSIFIED DATA Atomic Energy Act of 1954



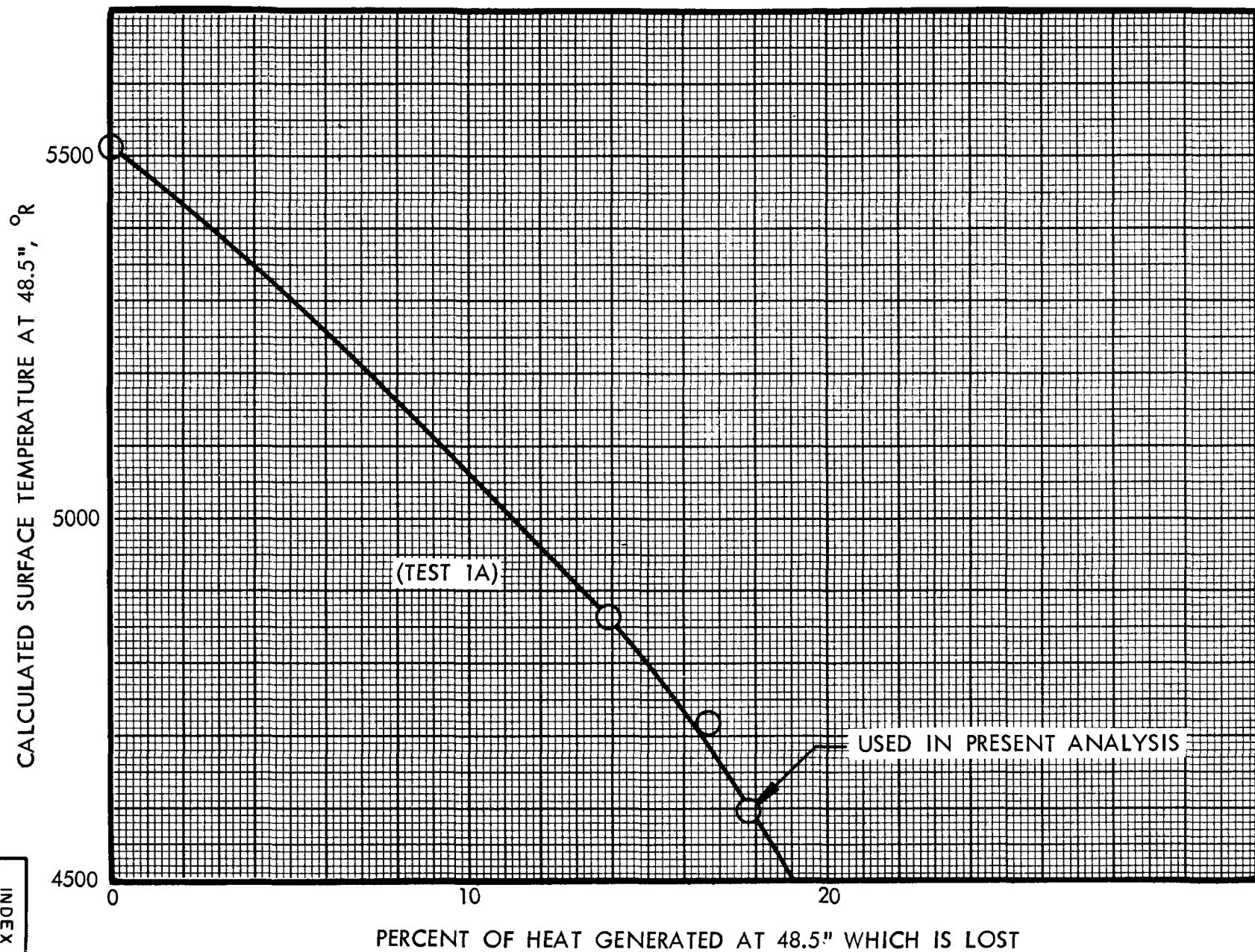
INDEX NO

FIGURE 7 NORMALIZED AXIAL HEAT GENERATION FOR ELECTRICAL HEATING

PREPARED BY	APPROVED BY	CURVE NO
QP	CS	597406

REFERENCE

Astronuclear



INDEX NO.

FIGURE 8

EFFECT OF ASSUMED HEAT LOSS ON CALCULATED SURFACE TEMPERATURE FOR A GIVEN HEAT INPUT

PREPARED BY

R.P.

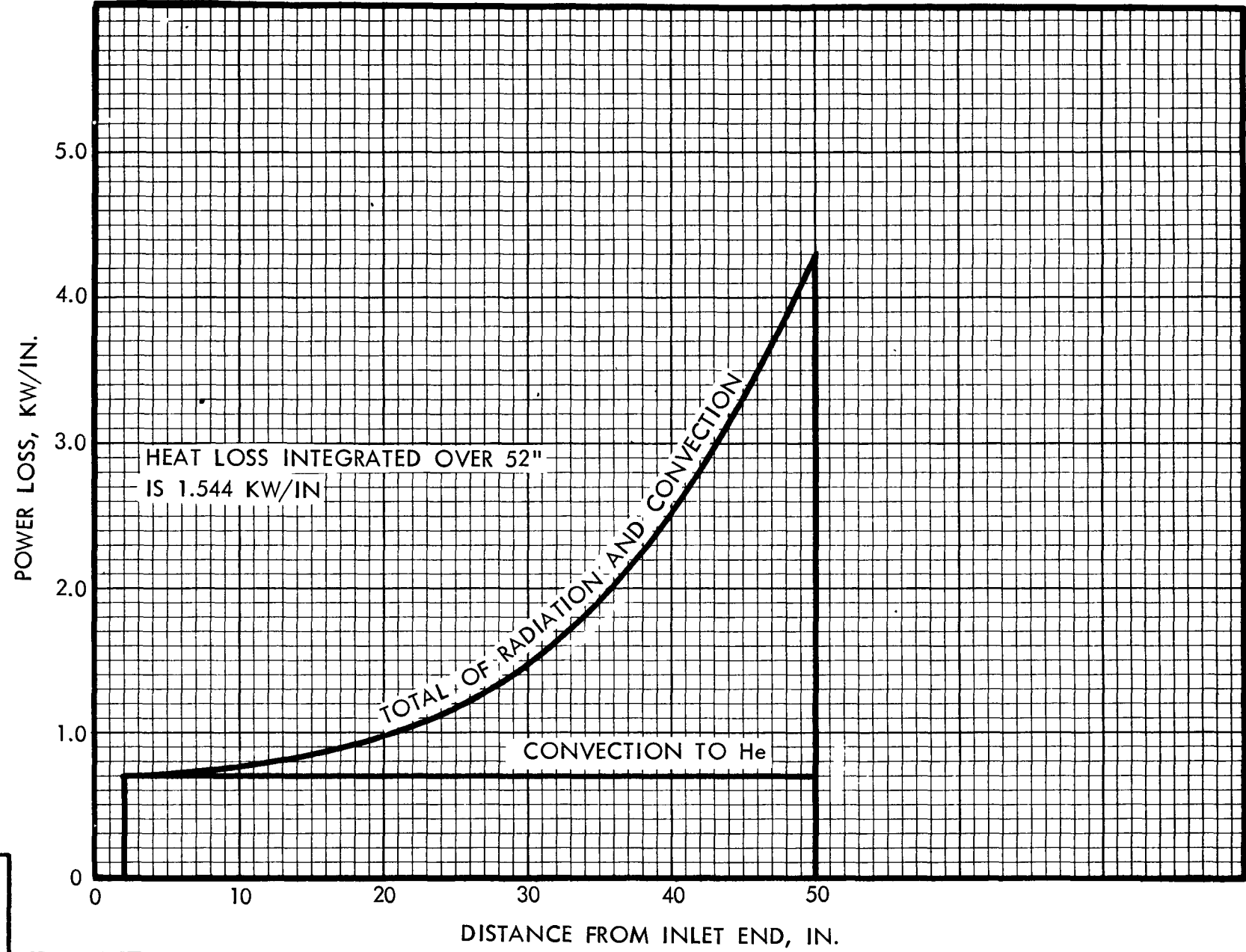
APPROVED BY

aj

CURVE NO.

5974051

REFERENCE



INDEX NO.

FIGURE 9

DISTRIBUTION OF HEAT LOSS FOR 4460 °R SET TEMPERATURE (TEST 1B)

PREPARED BY

ab

APPROVED BY

ab

CURVE NO.

597404A

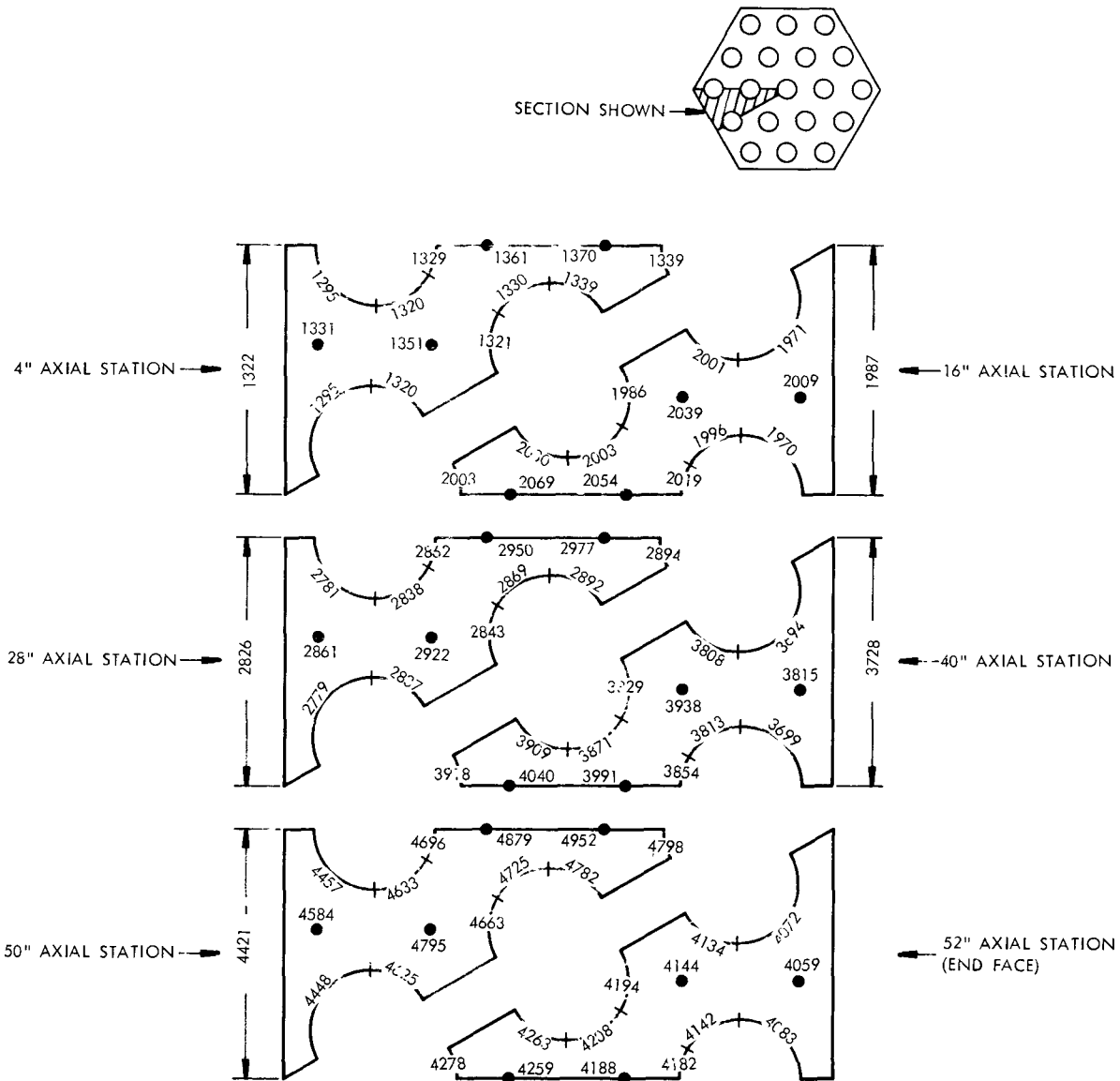


FIGURE 10

597383A

TEMPERATURE DISTRIBUTION AT AXIAL LOCATIONS FOR 4320 °R SET POINT
 (TEST 1C)

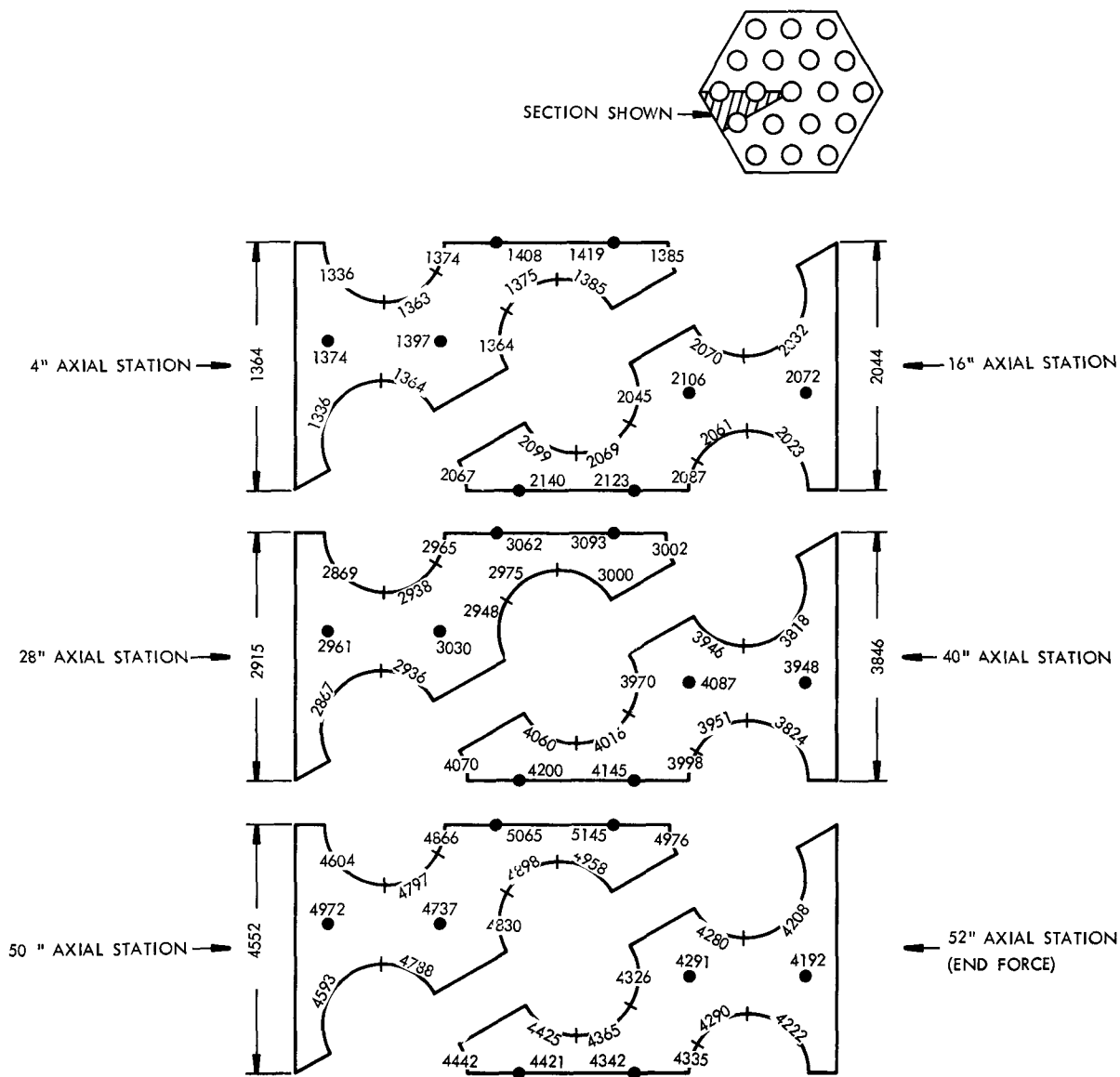


FIGURE 11

TEMPERATURE DISTRIBUTION AT AXIAL LOCATIONS FOR 4460 °R SET POINT
 (TEST 1B)

597384A

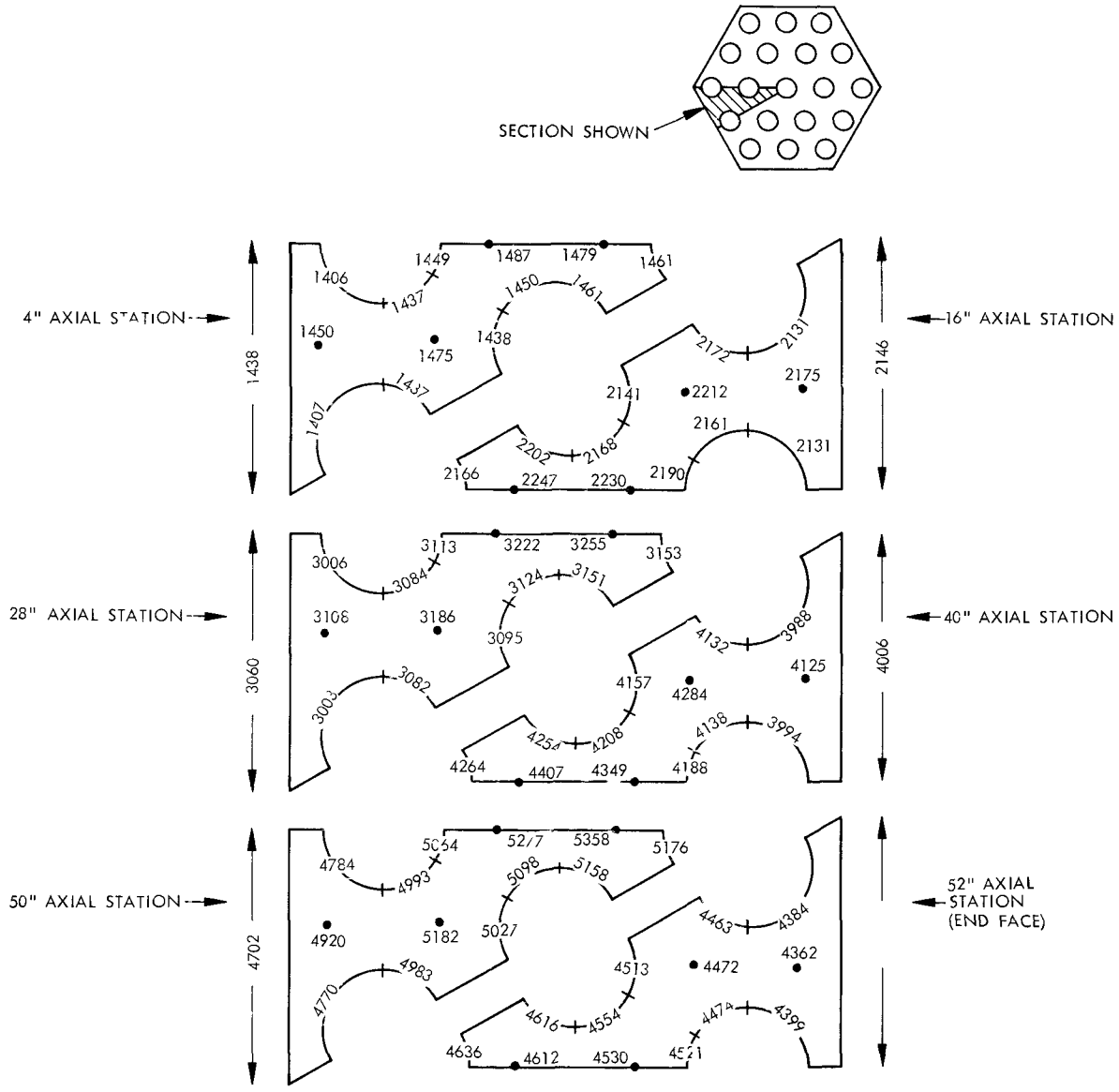
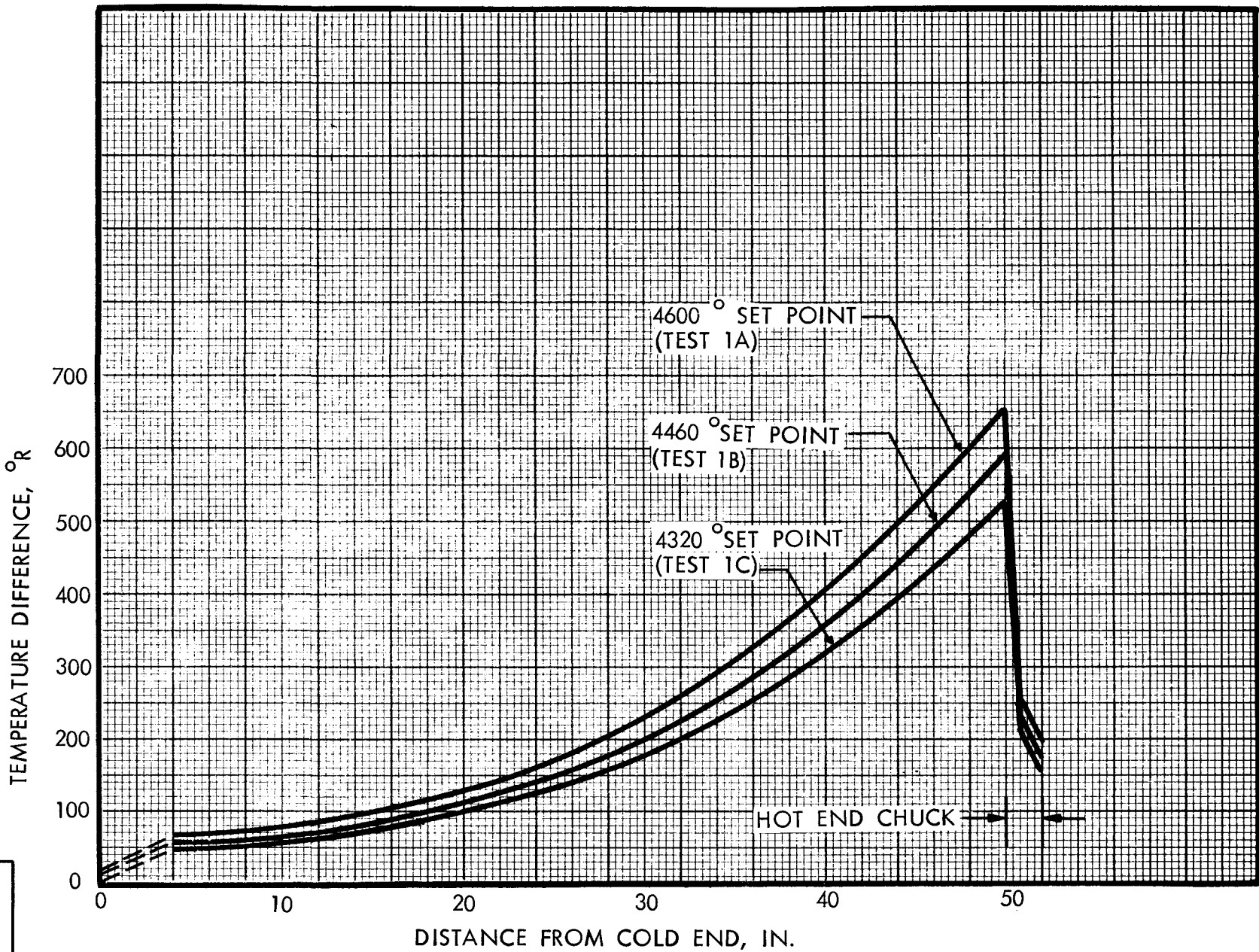


FIGURE 12

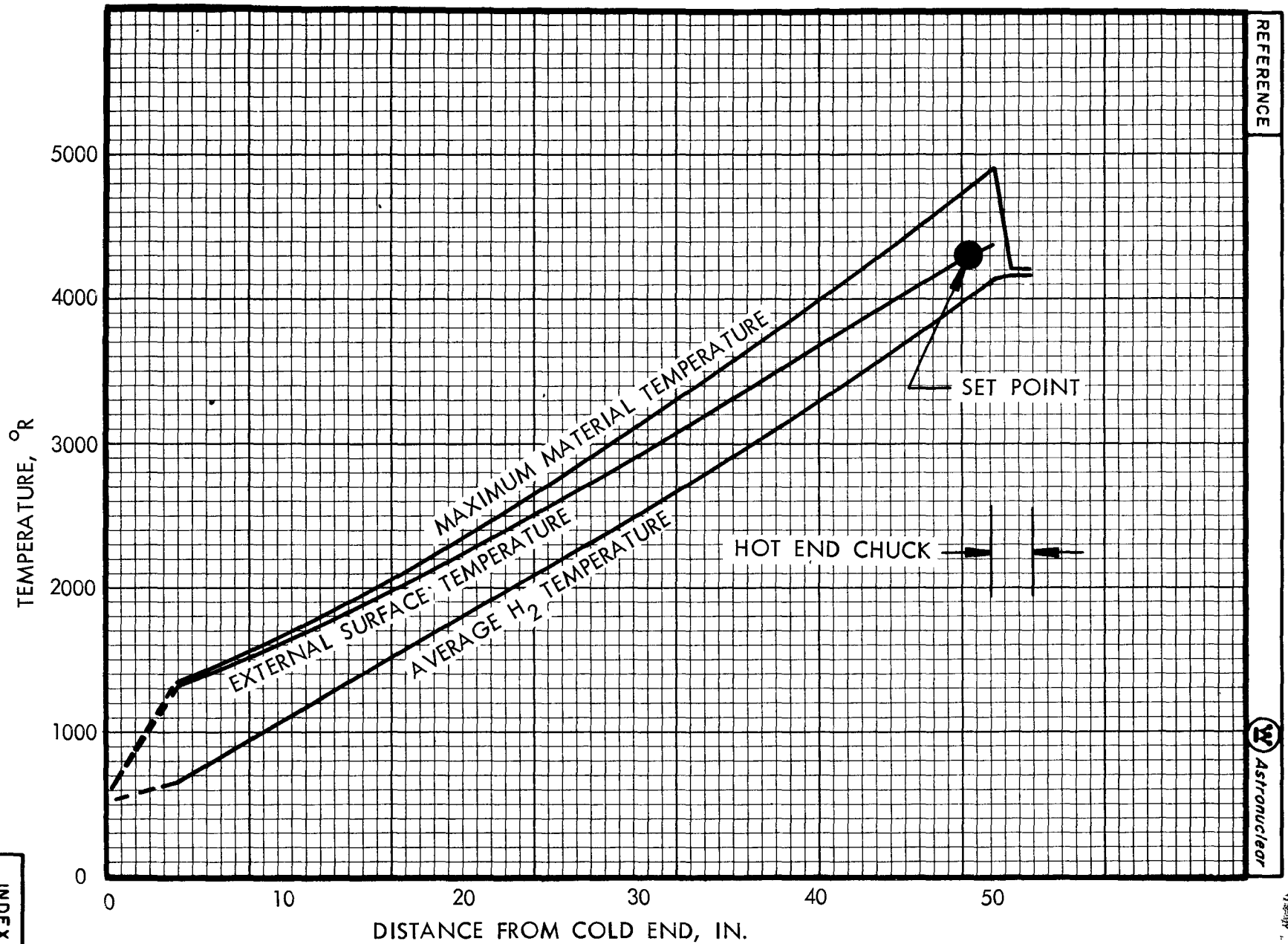
597386A

TEMPERATURE DISTRIBUTION AT AXIAL LOCATIONS FOR 4600 °R SET POINT (TEST 1A)



INDEX NO.

FIGURE 13	MAXIMUM CALCULATED TEMPERATURE DIFFERENCE ALONG THE ELEMENT	PREPARED BY	APPROVED BY	CURVE NO.
		<i>RP</i>	<i>RS</i>	594331



REFERENCE



INDEX NO.

FIGURE 14 CALCULATED AXIAL TEMPERATURE DISTRIBUTION FOR 4320 °R SET POINT (TEST 1C)

PREPARED BY

RP

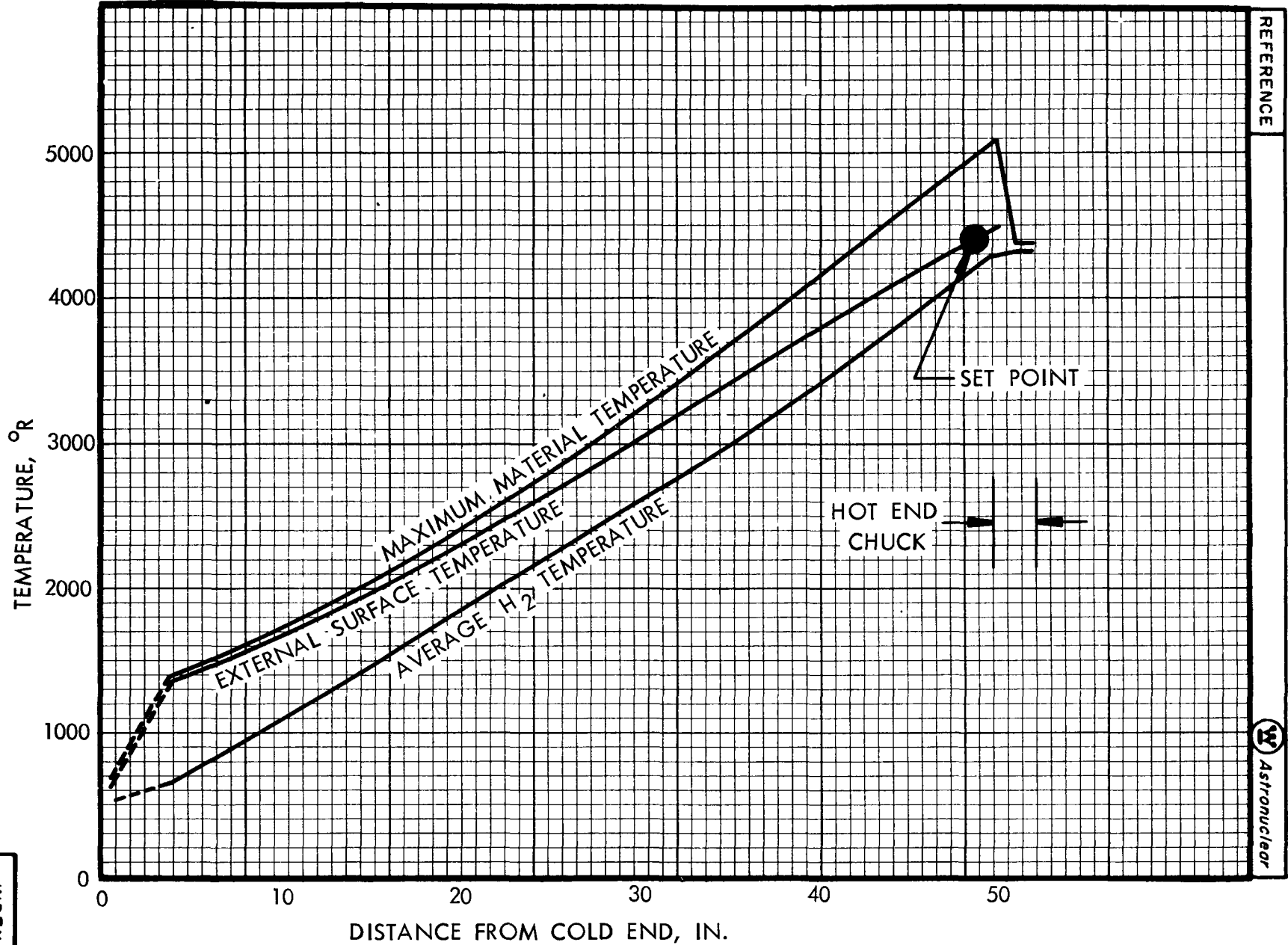
APPROVED BY

CB

CURVE NO.

597401 /-

INDEX NO.



REFERENCE

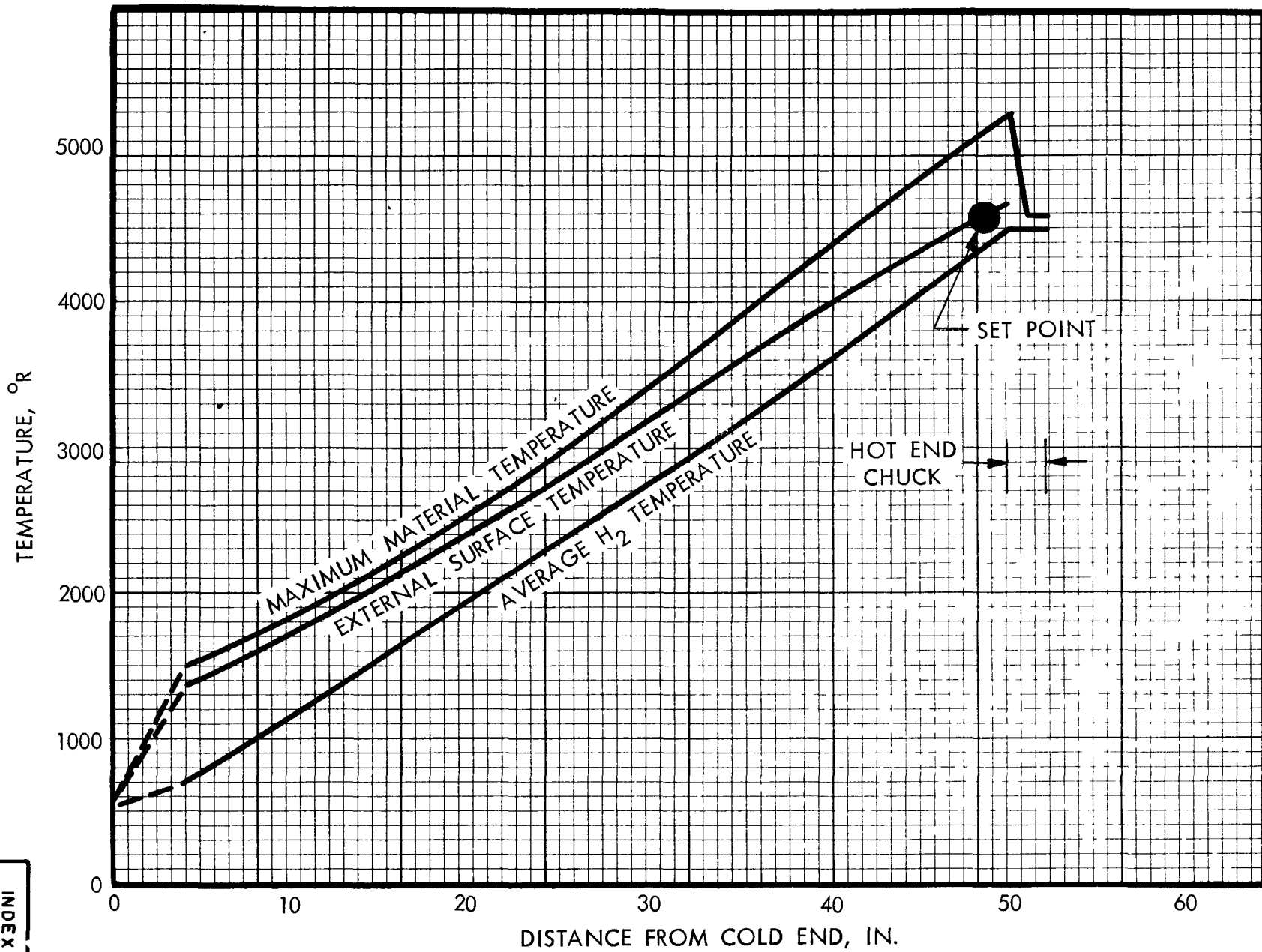


FIGURE 15 CALCULATED AXIAL TEMPERATURE DISTRIBUTION FOR 4460 °R SET POINT (TEST1B)

PREPARED BY	APPROVED BY	CURVE NO.
<i>RG</i>	<i>ab</i>	597402 A

REFERENCE

 Astronuclear



INDEX NO

FIGURE 16 CALCULATED AXIAL TEMPERATURE DISTRIBUTION FOR 4600 °R SET POINT (TEST 1C)

PREPARED BY	APPROVED BY	CURVE NO
<i>RD</i>	<i>ES</i>	3-1-54

CONFIDENTIAL RESTRICTED DATA Atomic Energy Act of 1954

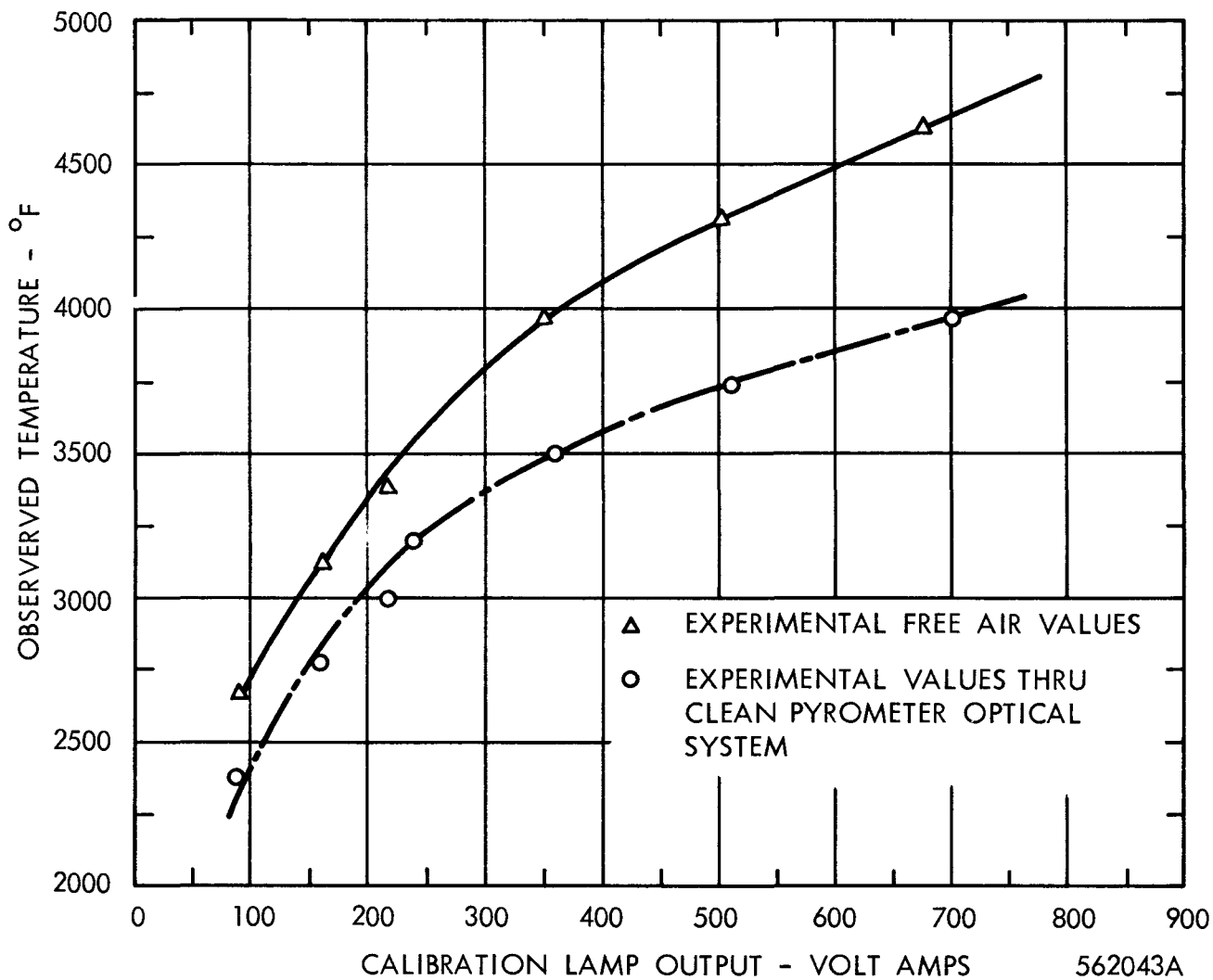
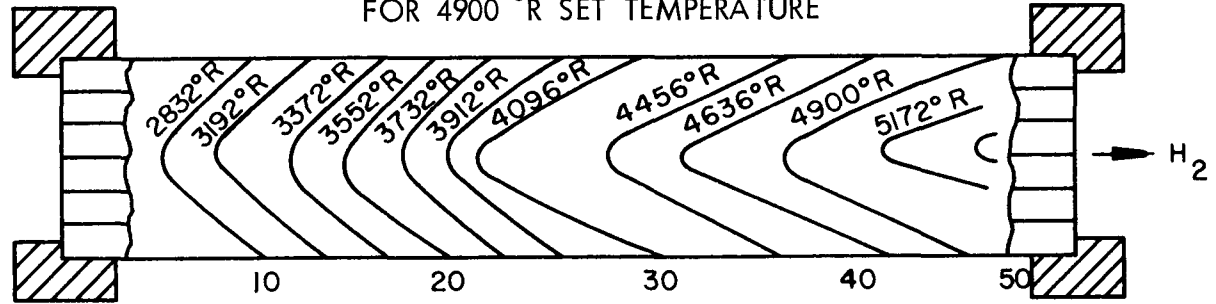


FIGURE 18 CALIBRATION OF OPTICAL PYROMETER

REFERENCE

ASTRONUCLEAR

TEMPERATURE GRADIENTS ESTIMATED
BY MATERIAL ANALYSIS
FOR 4900 °R SET TEMPERATURE



CALCULATED TEMPERATURE GRADIENTS
FOR 4460 °R SET TEMPERATURE, (TEST 1B)

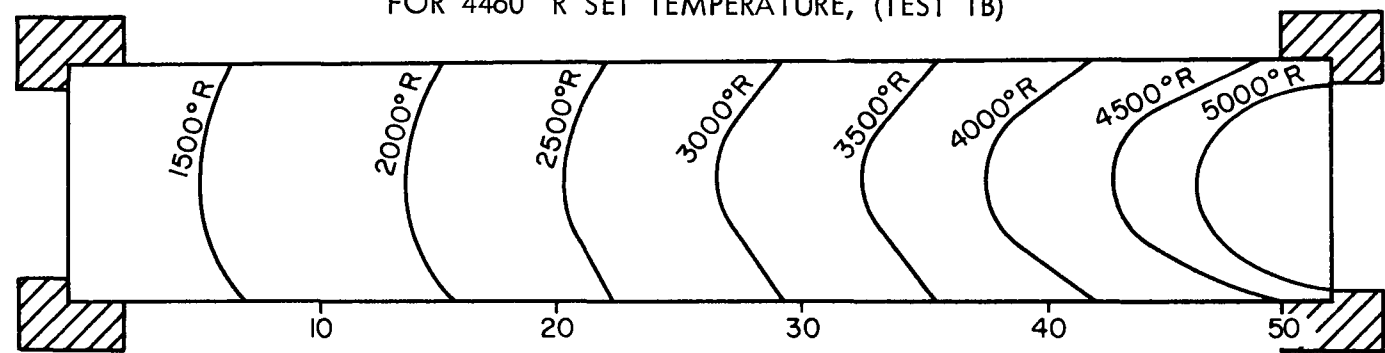
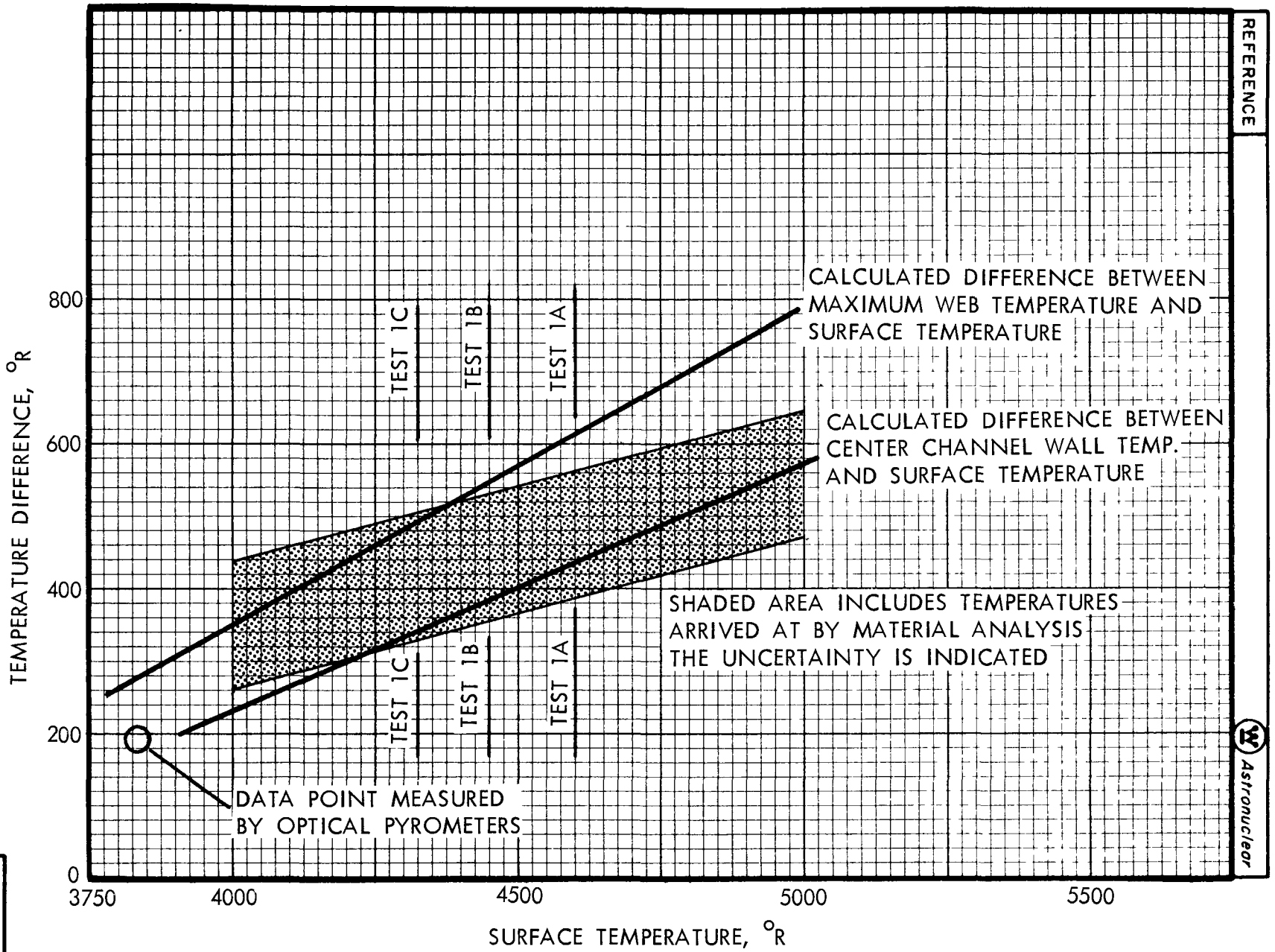


FIGURE 19 TEMPERATURE GRADIENT ON AN AXIAL CROSS SECTION OF A FUEL ELEMENT

INDEX NO.

PREPARED BY	APPROVED BY	CURVE NO
<i>JD</i>	<i>(Signature)</i>	537993

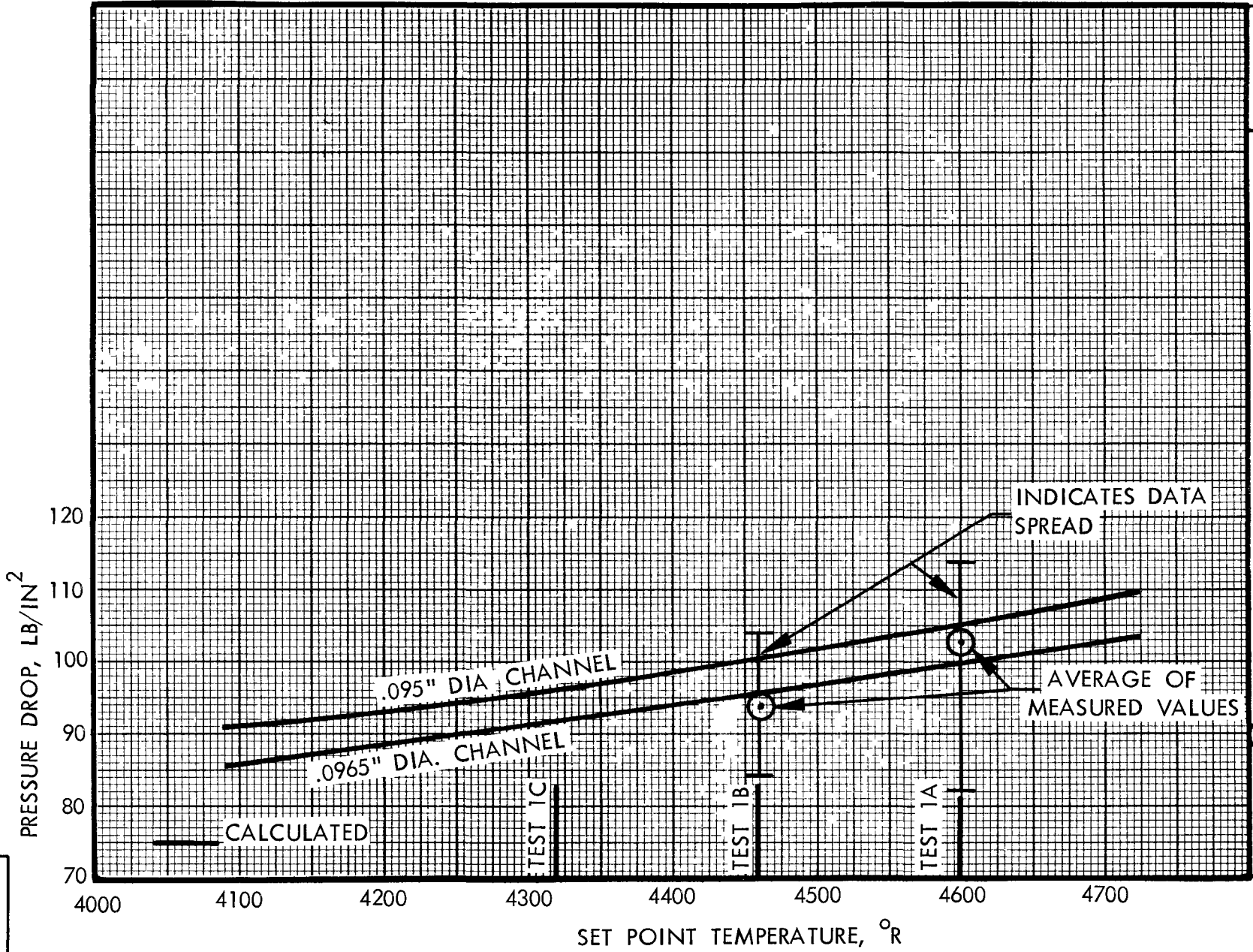


INDEX NO.

FIGURE 20 COMPARISON OF CALCULATED TEMPERATURE VARIANCE TO VARIANCE MEASURED BY MATERIAL ANALYSIS

PREPARED BY	APPROVED BY	CURVE NO.
<i>RP</i>		

REFERENCE



INDEX NO

FIGURE 21 COMPARISON OF MEASURED AND CALCULATED PRESSURE DROP

PREPARED BY *RP*

APPROVED BY *WJ*

CURVE NO 597396 A

CONFIDENTIAL RESTRICTED DATA

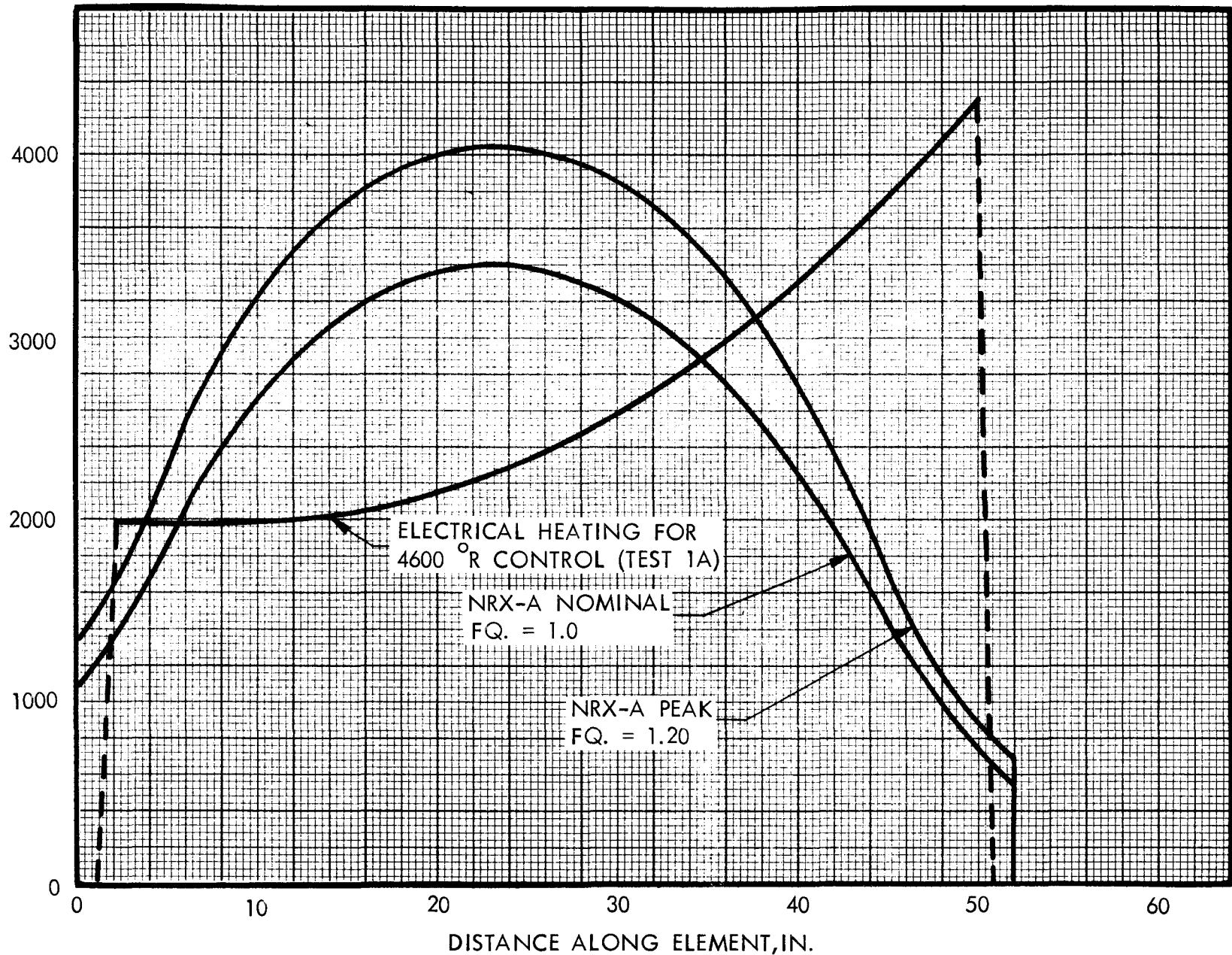
CONFIDENTIAL RESTRICTED DATA Atomic Energy Act of 1954

CONFIDENTIAL RESTRICTED DATA Atomic Energy Act of 1954

REFERENCE

 Astronuclear

HEATING RATE, WATTS/CM³



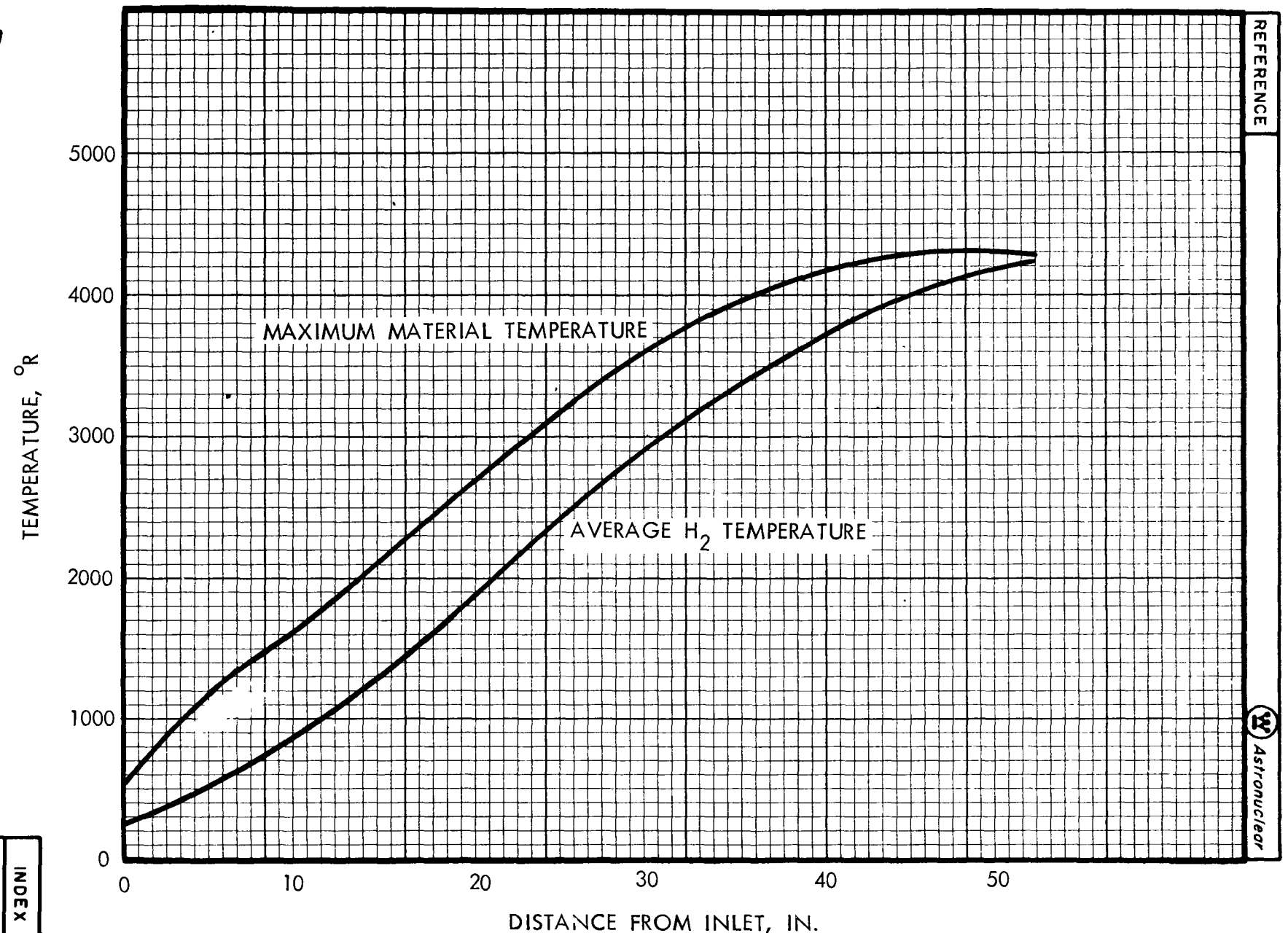
INDEX NO.

FIGURE 22 NRX-A HEATING RATES COMPARED TO ELECTRICAL HEATING AT 4600 °R SET POINT

PREPARED BY	APPROVED BY	CURVE NO.
<i>20</i>	<i>(signature)</i>	597390

CONFIDENTIAL REPRODUCED DATA

-41-



REFERENCE

ASTRONUCLEAR

CONFIDENTIAL REPRODUCED DATA

INDEX NO.

FIGURE 23 NRX-A DESIGN AXIAL TEMPERATURE DISTRIBUTION
 FQ = 1.0

PREPARED BY

20

APPROVED BY

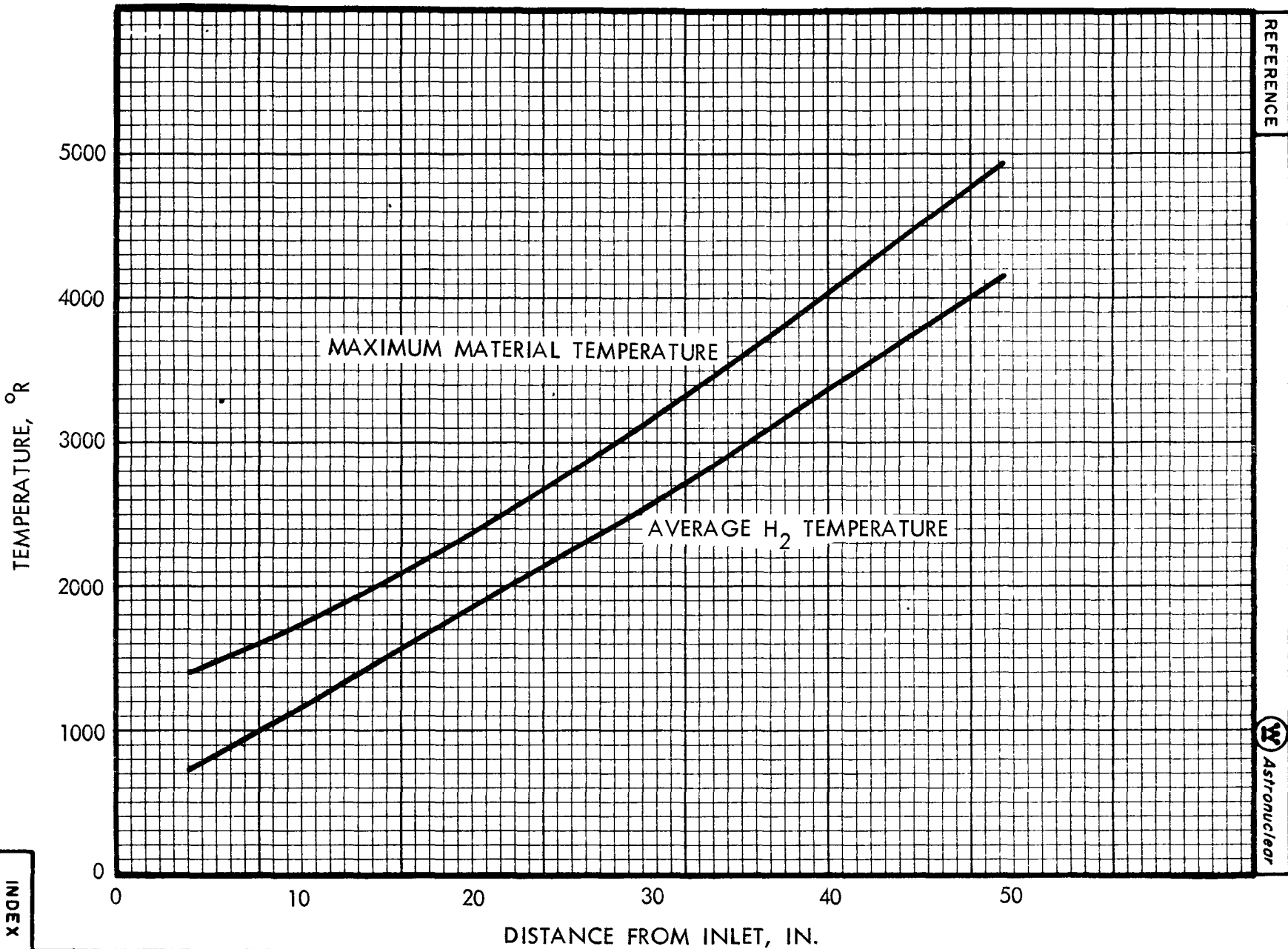
[Signature]

CURVE NO.

597389

CONFIDENTIAL UNCLASSIFIED DATA Atomic Energy

-42-



REFERENCE

 Astronuclear

CONFIDENTIAL UNCLASSIFIED DATA Atomic Energy

INDEX NO.

FIGURE 24 COMPONENT TEST AXIAL TEMPERATURE DISTRIBUTION FOR 4320 °R SET TEMPERATURE (TEST 1C)

PREPARED BY
LD

APPROVED BY
LD

CURVE NO.
597388

~~CONFIDENTIAL~~
~~RESTRICTED DATA~~
Atomic Energy Act, 1954

-43-

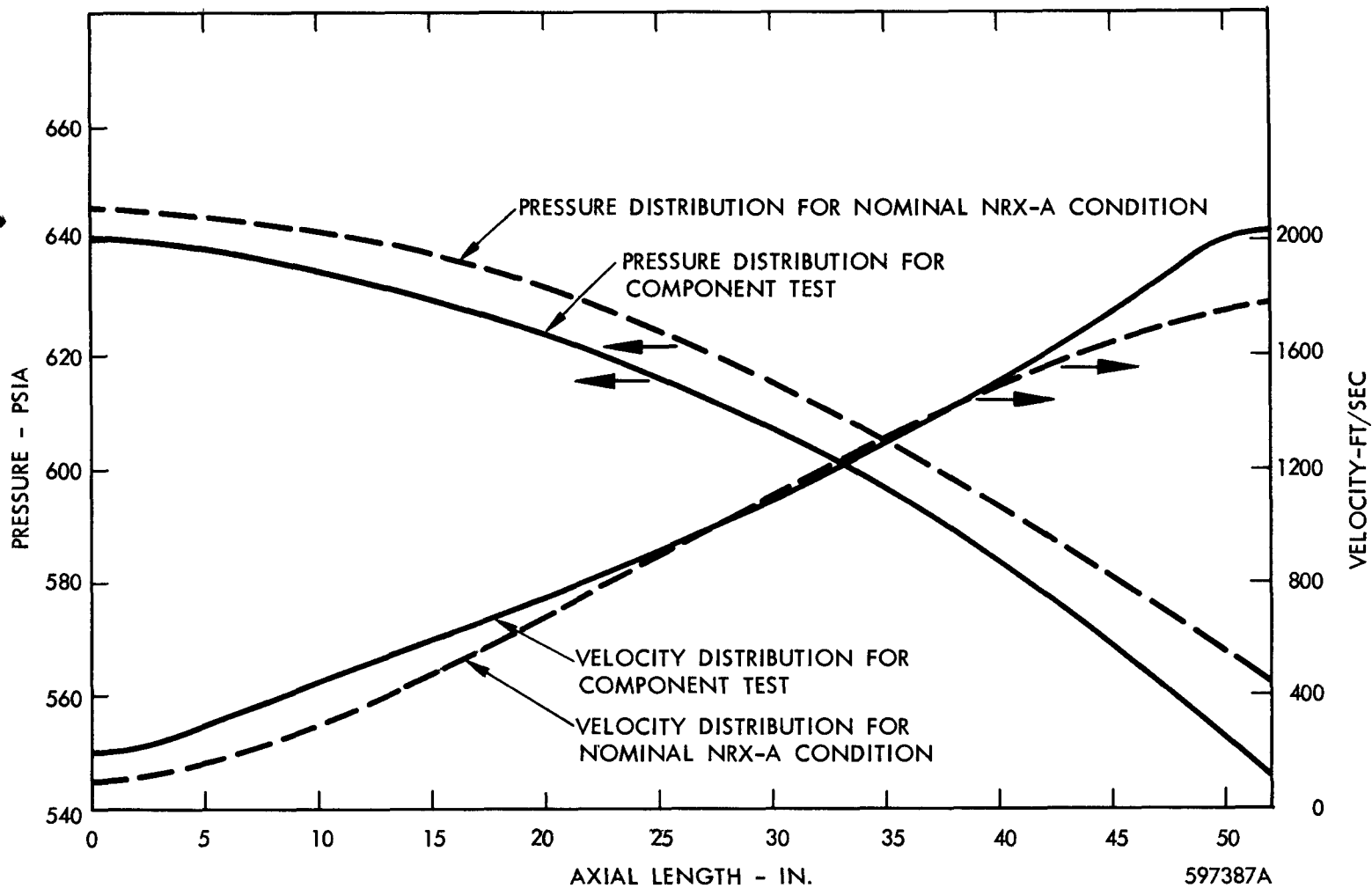


FIGURE 25 VELOCITY AND PRESSURE DISTRIBUTION FOR NOMINAL NRX-A

597387A

~~CONFIDENTIAL~~
~~RESTRICTED DATA~~
Atomic Energy Act, 1954

